Neuroscience Research, 9 (1990) 1–21
Elsevier Scientific Publishers Ireland Ltd.

主論文 (1)

NEURES 00388

Review Article

Recent progress in the use of the technique of non-radioactive in situ hybridization histochemistry: new tools for molecular neurobiology

Hiroshi Kiyama [1,2], Piers C. Emson [1] and Masaya Tohyama [3]

[1] *MRC Group, Institute of Animal Physiology and Genetics Research, Babraham, Cambridge (U.K.) and* [2] *Department of Neuroanatomy, Biomedical Research Center and* [3] *Department of Anatomy, Osaka University Medical School, Osaka (Japan)*

(Received 29 March 1990; Accepted 25 April 1990)

Key words: Alkaline phosphatase; Neurotransmitter; Gene expression; Double labelling; Cell culture; Human tissue; Peripheral nervous system

SUMMARY

Recent developments in DNA and oligonucleotide chemistry have made it possible to modify nucleotides and link quite complex molecules to the modified nucleotides. These advancements in DNA chemistry provide a number of possibilities for labelling oligonucleotide probes for DNA or RNA detection by non-radioactive methods. Over the years a number of non-radioactive detection systems for mRNA or chromosomal DNA have been developed. As reporter molecules, biotin, acetylaminofluorene, dinitrophenol, digoxigenin, sulfonized nucleotides, and mercury have been used and may be detected with a variety of high-affinity detectors, e.g. avidin (in the case of biotin) or antibodies specific to digoxigenin. These various 'indirect methods' of detection have used a number of chemical amplification procedures in attempts to improve their sensitivity. However, the sensitivity of these methods is often less than that of conventional radioactive methods. A sensitive non-radioactive technique would have a number of advantages over the complex and specialized radioactive in situ hybridization methods. In our laboratory we have recently found that simple enzyme-labelled probes provide excellent sensitivity (equivalent to that found with radioactive methods) and substantially improved cellular resolution. In this article, we describe the principle of the method and illustrate some applications of this novel non-radioactive in situ method.

CONTENTS

Correspondence: Dr. H. Kiyama, Department of Neuroanatomy, Biomedical Research Center, Osaka University Medical School, 4-3-57 Nakanoshima, Kitaku, Osaka 530, Japan.

1. INTRODUCTION

The nervous system is unique among body organs in the complexity of its organization and chemistry. Individual nerve cells lying adjacent to each other may, for example, contain several putative neurotransmitters, and express a variety of different receptors. This diversity in biochemical composition of the cells means that any analysis of gene expression should both be carried out with a high spatial resolution and allow a detailed morphological approach.

Recent rapid progress in the field of molecular biology has provided the morphologist with a new range of DNA probes with which to localize a mRNA signal within a cell or tissue section[22,46,56,58]. This technique called 'hybridization histochemistry' or 'in situ hybridization' allows the neuroanatomist to follow changes in gene expression at the single-cell level during development, or to analyze changes in cellular signals occurring during physiological or pharmacological experiments.

Immunohistochemistry and in situ hybridization histochemistry, which visualize respectively the translated protein product and the transcribed mRNA or chromosomal DNA, represent major developments in the field of morphological analysis. The widespread use of antibody probes in neurobiology has provided an enormous amount of information about the chemical composition of a variety of cell types. The technique of in situ hybridization, however, not only offers a unique way of confirming many of these histochemical data but is also a better index of synthetic activity. This is because, in general, changes in the rate of mRNA transcription are much more rapid (hours) than those seen for the translated gene product (i.e. protein or peptide) which may turn over much more slowly (days). It has thus become feasible to detect, at the single-cell level, which neurons or neuronal systems are activated by a particular stimulus. Moreover, using immunohistochemistry, it is often impossible to distinguish between substances whose amino acid compositions are very similar (e.g. α- and β-CGRP), whereas the use of specific probes in in-situ hybridization makes it possible to differentiate even closely related signals[39]. The non-radioactive technique we describe here provides us with a novel tool to investigate the control of gene expression and enables us to approach a range of difficult problems including, for example, the changes in gene expression underlying the formation of the memory trace.

2. CONVENTIONAL IN SITU HYBRIDIZATION METHODS AND THEIR LIMITATIONS[54,56,58]

In order to detect a specific mRNA or chromosomal DNA of interest, a probe is required which has a sequence complementary to that of the target. Three types of probes

are available: (a) complementary DNA (cDNA) fragments which are cut out from plasmid vector, (b) complementary RNA (cRNA) which has been ligated into a plasmid vector containing a bacteriophage RNA polymerase transcription site (either SP6 or T7), and (c) specifically synthesized anti-sense oligonucleotides which are synthesized by an automated DNA synthesizer. The radioisotopically labelled probe is hybridized to the target mRNA or DNA and is usually visualized by conventional autoradiography. These probes are routinely labelled with a radioisotope such as ^{32}P, ^{35}S or ^{3}H. Amongst the radioisotopes available, ^{35}S is usually the most popular, because it provides a good balance between autoradiographical resolution (the signal is well localized within a few microns of the decay event) and a reasonable energy level allowing convenient exposure times to be used (1–4 weeks on average). The lower-energy radioisotopes (^{3}H) have a higher resolution, but require much longer exposure times, because the signal is less energetic.

Two methods of autoradiographical detection have routinely been used to visualize a target mRNA or chromosomal DNA. One is film-based autoradiography whereby a sheet of autoradiography film is placed in direct contact with the hybridized slides, exposed for an optimal period of time to detect the isotopic decay, and then developed. The second method is emulsion autoradiography in which a section which has been hybridized with a radiolabelled probe is coated with a layer of emulsion, exposed in the dark for several weeks, and then developed. Film-based autoradiography is generally easier to carry out and is more suitable for quantitative analysis, but emulsion-autoradiography has a much higher cellular resolution. Both techniques require long exposure times, generally have low resolution, and give relatively high backgrounds. Also it is technically very difficult to apply the radioactive method for electron-microscopic analysis or to use it for visualization of more than one mRNA per section. Moreover, the use of radioisotopes requires specialized equipment and produces radioactive waste which has to be disposed of. For all these reasons, a sensitive and reliable method of non-radioactive in situ hybridization would represent a substantial breakthrough in the study of gene expression.

3. NON-RADIOACTIVE METHODS

In order to resolve these autoradiographical problems, a number of workers have sought alternative labelling methods and have developed methods not requiring radioisotopes (Table I). Improvements in the chemistry of nucleic acids have enabled a number of modified bases to be produced to which a number of enzyme groups can be directly attached as reporter molecules[1,15,47]. These modified nucleic acids often have a primary aliphatic amino group which is much more nucleophilic than those present on the heterocyclic bases of nucleic acid, and can be selectively reacted with a variety of suitable reagents. It has also been found that the C-5 of the pyrimidine base or the C-8 of the purine base is a good site for the attachment of a reporter molecule or label, as this results in the least amount of interference with hybridization[15]. It is also possible to incorporate a pre-modified base into a probe by an enzymatic reaction or with a DNA synthesizer. A variety of strategies have been used to seek suitable labelling groups. In principle, instead of the radioisotope, a small chemical reporter molecule is attached to a probe, and is localized by a suitable 'detector' which should have both high affinity and specificity. This type of method whereby the original reporter molecule (e.g. biotin) is amplified by the build-up of a complex product can be termed an 'indirect method'[2,7,43] (Table I). An important criterion for selecting a good reporter molecule for an indirect method is that it should be small and have the ability to penetrate into a tissue. Subsequent detection then

TABLE I

NON-RADIOACTIVE REPORTER MOLECULES FOR LABELLING OF PROBES

INDIRECT METHOD		
Reporter molecule	*Detector*	*References*
Acetylaminofluorene (AAF)	Antibody	Tchen et al.[55] Landegent et al.[30]
Biotin		
Biotin-dUTP	Streptavidin (antibody)	Langer et al.[32] Leary et al.[33]
5′-Biotin	Streptavidin (antibody)	Agrawal et al.[1]
Photobiotin	Streptavidin (antibody)	Forster et al.[12]
Digoxigenin (-dUTP)	Antibody	Heiles et al.[16]
Dinitrophenol (DNP)	Antibody	Shroyer et al.[48]
Photo-DNP	Antibody	Keller et al.[24]
Br-guanine(C8)-DNP	Antibody	Keller et al.[23]
Mercury	HS-hapten and antibody	Dale et al.[8] Hopman et al.[19]
Sulfonation	Antibody	Sverdlov et al.[53] Poverenny et al.[42]
DIRECT METHOD		
Reporter molecule	*Modification of probe*	*References*
Fluorescent primer	5′-Amino	Smith et al.[49]
Enzyme	Amino-thymidine (C-5)	Ruth et al.[47]
(alkaline phosphatase)		Jablonsky et al.[21]
	5′-Amino	Li et al.[36]
	3′-Amino-SH	Chu et al.[6]
	Amino-cytosine (C-5)	Urdea et al.[57]

requires a highly sensitive, easily amplified detection system. So far, biotin,[2,7,12,13,20,32,33,35,41], digoxigenin[3,14,16], dinitrophenol[23,24,48,60], mercury[8,17,18,19], acetylaminofluorene[10,30,31,55], and sulfonized nucleotide[34,40,53] have been tested as potential reporter molecules for use in in-situ hybridization (Table I). Amongst these reporters, the most popular has been biotin, although more recently digoxigenin has become widely used. Biotin is a small molecule (MW = 244) which can be detected by avidin which has a very high affinity for the molecule ($Kd = 10^{-15}$ M), meaning that this reaction is essentially specific. Probes can easily be labelled with biotin, using biotinylated nucleotides in exactly the same way as radioactive nucleotides are incorporated into DNA or RNA. In this chapter, we describe briefly the basic methodology of some earlier non-radioactive methods using biotin as an example of the use of a non-radioactive reporter molecule.

All types of probes, whether cDNA, cRNA or oligonucleotides can be labelled with biotin. A biotinylated nucleotide is routinely used in which a biotin molecule is cross-linked to a nucleotide via a linker arm. Various kinds of biotinylated nucleotides are now commercially available, including, for example, 11-, 16- and 21-biotin dUTP (Fig. 1a). These biotinylated nucleotides can be incorporated into the relevant probe enzymatically, using nick translation, primer extension, 3′- and 5′-end labelling, the RNA polymerase extension method or by using the polymerase chain reaction (PCR).

Another method of biotin-labelling is to use photobiotin which carries a photosensitive base group which can be crosslinked by irradiation with strong light to DNA or RNA

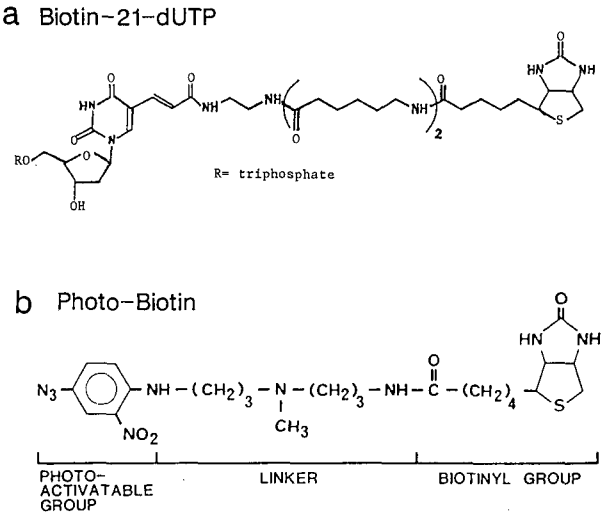

Fig. 1. The structures of biotinylated nucleotide and photobiotin. (a) The structure of biotin-21-dUTP. A biotin is linked to dUTP via a long linker arm. This modified nucleotide can be incorporated into a probe enzymatically. (b) The structure of photobiotin. A biotin molecule is linked to a photoactivatable group via a linker arm. The photoactivatable base can be bound to the probe by irradiation with strong light.

probes[12]. The photoactive base is located at the end of the linker arm in photobiotin which is connected to a biotin group at the other end (Fig. 1b). As described, irradiation with a strong light source will link the photobiotin to a DNA or RNA probe; however, the precise reaction of the photoactive base and the preferred site of attachment to the DNA or RNA probe are unknown. The advantage of photobiotin is its simplicity, as it does not require an enzymatic reaction, and it is easy to check that the labelling has been carried out successfully by following the change in color of the probe after ethanol precipitation. Unincorporated free photobiotin remains in the ethanol phase, and the labelled probe, which is precipitated by the ethanol, should have a brown color.

Biotin-labelled probes can be detected by a range of different methods. These methods are summarized schematically in Figure 2. Biotin on a DNA or RNA probe can be detected by avidin, or an anti-biotin antibody, and finally visualized by an enzymatic color reaction [using horseradish peroxidase (HRP) or alkaline phosphatase] or fluorescence. Other reporter molecules such as digoxigenin are usually detected by the use of specific antibodies and visualized using suitably labelled second antibodies. In order to improve the sensitivity of the biotin or digoxigenin methods, a number of chemical amplification systems have been tried. However, the sensitivity of all these probes which are visualized 'indirectly' and require signal amplification is still less than the best radioactive probes. Some mRNAs which are found in high copy numbers in specific cells: e.g., the neurohypophysial hormone mRNAs in the hypothalamus or virus mRNA in infected tissue are readily detectable by these non-radioactive methods[2,13]. However, other mRNAs which are not so abundant have proved very difficult to detect with existing non-radioactive methods. In fact, although the above non-radioactive methods have some advantages, they are not widely used in the study of neuronal gene expression because of their low sensitivity. For this reason a reliable and sensitive non-radioactive method was required, and we have found that a non-radioactive in situ method using an enzyme-

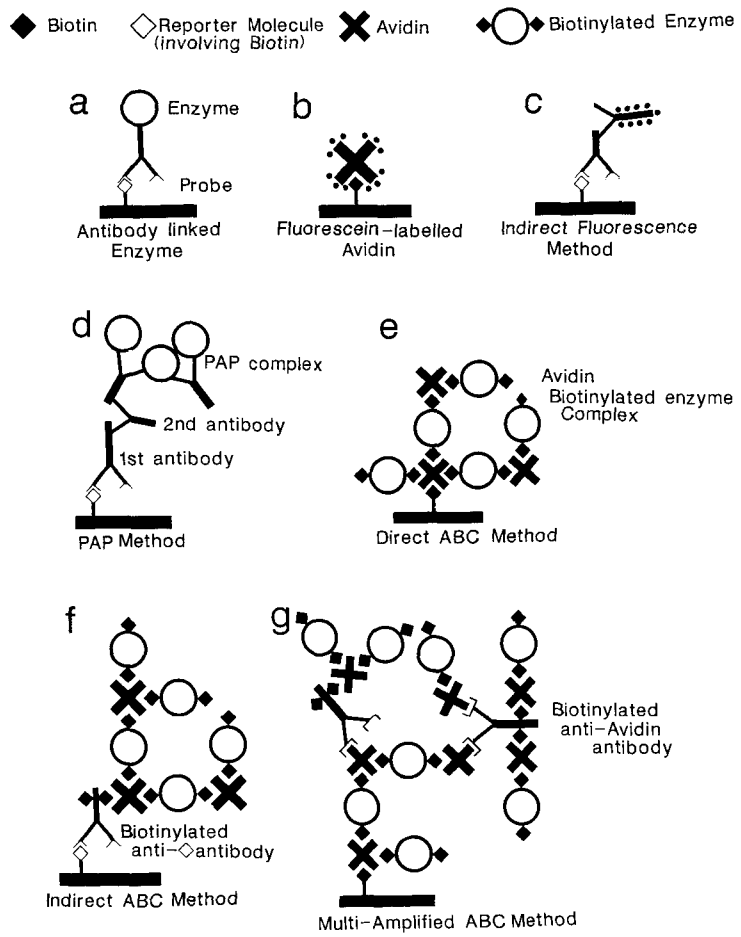

Fig. 2. Indirect methods of visualizing reporter molecules linked to oligonucleotide probes. (a) Reporter molecule involving biotin is detected by the anti-reporter molecule antibody which is linked to an enzyme, such as alkaline phosphatase or horseradish peroxidase. (b) Fluorescence-labelled avidin or streptoavidin is used as a detector of biotin. (c) The primary antibody is specific against the reporter molecule and is visualized using a fluorochrome-labelled 2nd antibody. (d) The reporter molecule is detected using the concentrated immunohistochemical PAP method. (e) The biotin reporter molecule is detected using an avidin–biotin enzyme complex. Alkaline phosphatase or HRP may be used as the enzyme. (f) The reporter molecule is initally reacted with a biotinylated anti-reporter molecule antibody and then detected with an avidin–biotin enzyme complex. (g) The biotin reporter molecule linked to the probe is first detected by an avidin–biotin enzyme complex. In order to increase the enzyme amplification, a biotinylated anti-avidin antibody is used as a bridge molecule just like the 2nd antibody in the PAP method. Finally another avidin–biotin enzyme complex may be attached, as the biotinylated anti-avidin antibody has multiple binding sites for avidin.

labelled oligodeoxynucleotide probe gave excellent results. This method has a sensitivity comparable to that of the best radioisotopic methods (see below).

4. THE USE OF ENZYME-LABELLED OLIGODEOXYNUCLEOTIDE PROBES IN NON-RADIOACTIVE IN SITU HYBRIDIZATION

4.1. Advantages

As noted earlier, we have found that simple enzyme-linked oligonucleotide probes labelled with HRP or alkaline phosphatase are the most suitable for use in non-radioac-

tive in situ hybridization. This method is a 'direct method', i.e. there are no additional amplification steps before the detection of the enzyme reporter molecule[21,43,45] (Table I). Most of the earlier literature derived from immunohistochemical studies had suggested that 'indirect' methods have much higher sensitivity than simpler 'direct methods', for example the PAP method versus a single enzyme-labelled antibody[51]. It had therefore been thought that a reliable chemical amplification step would be necessary for the detection of a non-radioactive mRNA signal.

In the 'direct' method, the 5′- and 3′-terminal fluorochrome labels we tested first did not give acceptable results[4]. However, we have found now that enzyme-labelled probes, particularly those carrying the robust enzyme alkaline phosphatase, give excellent signal detection usually without problems with washing temperatures or steric hindrance[21,26,27,29]. It is also critical that the reporter molecule should retain activity in the hybridization buffer, tolerate high wash temperatures and not affect the kinetics of hybridization. Although, as expected, it was found that oligonucleotide probes carrying a large enzyme such as alkaline phosphatase have a melting temparature some 10°C lower than the equivalent underivatized oligonucleotide probes on membranes[21], this was not a problem for in situ hybridization histochemistry because washing and hybridization conditions are routinely performed at lower temperatures. As noted, the sensitivity of these enzyme-labelled probes is comparable and sometimes better than conventional radiolabelled probes. This high sensitivity is due to both the high resolution obtained and the very low background signal observed. As the background is low, it is very easy to identify whether a weak signal is present within a single cell. This method, like the radioactive one, is direct and quantification of an mRNA signal is possible. It is also more reliable and reproducible than other non-radioactive methods in which the original small signal has to be greatly amplified. During these amplification stages, the number of possible errors increases rapidly and may deviate widely from the original signal. A final, and perhaps the most telling advantage of this method, is that it is *much simpler* and *quicker* than all other non-radioactive and radioactive in situ hybridization methods so far described.

4.2. Methodology

4.2.1. Structure and preparation of the probe A single alkaline phosphatase molecule is cross-linked to a single modified base which carries a linker arm[47]. This modified base is included during the synthesis of the oligonucleotide. The modified base is incorporated directly into the automated synthesis carried out on a DNA synthesizer (Fig. 3a). Alkaline phosphatase is cross-linked to the primary amine group on the linker arm using an amine-reactive bifunctional cross-linker such as disuccinimidyl suberate (DSS) (Fig. 3b). The alkaline phosphatase–oligodeoxynucleotide conjugate can then be separated by gel filtration and anion-exchange chromatography. Briefly the alkaline phosphatase–oligodeoxynucleotide conjugate and free alkaline phosphatase are separated from free oligodeoxynucleotide by filtration through a Biogel P-100 column, for example. Then the conjugate is separated from free alkaline phosphatase by DE52 anion exchange chromatography with a gradient of NaCl concentration (0–1 M). The free alkaline phosphatase comes first and then conjugate comes off. The fraction which contains conjugate or free alkaline phosphatase can be identified by the ratio of A_{260}/A_{280}, and the activity of alkaline phosphatase can be assayed spectrophotometrically by the hydrolysis of *p*-nitrophenyl phosphate at 405 nm (for this method, see Jablonsky et al.[21]).

4.2.2. Hybridization and color reaction Although a variety of methods for hybridization can be used for this type of novel probe, the following procedure is recommended

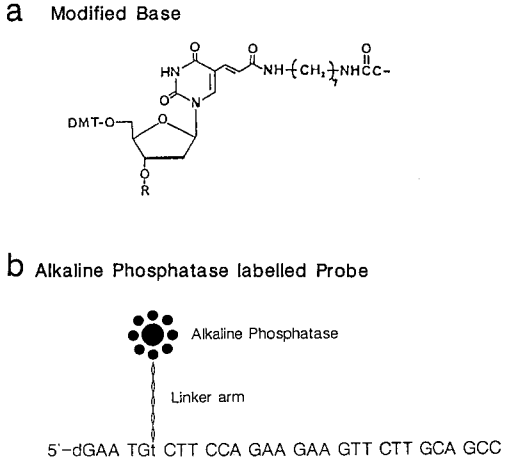

Fig. 3. Structure of an enzyme-linked probe. (a) A nucleic acid which has a linker arm and a primary amine group at the top of the linker arm is synthesized so as it may be used for attachment of an enzyme. (b) Modified nucleic acids are automatically incorporated into the probe by a DNA synthesizer and then labelled with the enzyme by cross-linking it to the amine group on the linker arm.

and works well in our hands:

(1) Fresh frozen sections are cut on a cryostat (5–20 μm).
(2) The sections are then fixed for 30 min in 4% paraformaldehyde in 0.1 M PB (pH 7.5).
(3) Sections are then washed with PBS for 10 min to remove the fixative.
(4) Sections are pretreated with 0.25% acetic anhydride in 0.1 M triethanolamine and 0.9% NaCl for a further 10 min.
(5) After the pretreatment, the sections are dehydrated with ethanol (70% up to 100%).
(6) Delipidated with chloroform for 10 min.
(7) Washed again with absolute ethanol.
(8) Hybridized in hybridization buffer at 37°C overnight. The hybridization buffer contains: 4 × SSC, 50% formamide, 1 × Denhardt's, 500 μg/ml salmon testis DNA, 10% dextran sulfate and probe (1–5 fmol/μl).
(9) After hybridization, sections are washed with 1 × SSC at room temperature to remove the hybridization solution, and then taken through a number of increasingly stringent washes (e.g., 4 times washes with 1 × SSC or 0.5 × SSC at 55°C each for 15–20 min).
(10) Following the washes, the sections are incubated in 0.1 M Tris–HCl (pH 7.4)/0.9% NaCl for 30 min.
(11) Sections are then incubated in 0.1 M Tris–HCl (pH 9.5)/0.1 M NaCl, 0.05 M $MgCl_2$ for 10 min.
(12) Sections are incubated in substrate solution at room temparature overnight in the dark to visualize the sites of hybridization. The substrate solution used consists of nitroblue tetrazolium (NBT) 340 μg/ml and 5-bromo-4-chloro-3-indolyl phosphate (BCIP) 170 μg/ml in buffer (11)[9,59].
(13) The color reaction is stopped after a suitable time with 10 mM EDTA (for 30 min).
(14) Finally sections are mounted under cover slips with 10 mM Tris–HCl (pH 7.4) containing 50% glycerol and 10 mM EDTA.

Steps (1)–(9) are equally suitable for use with radioactive probes (whether cDNA or oligo probes).

One of the advantages of alkaline-phosphatase-linked probes is the color of the final product which can be selected from red, blue, black or purple-brown depending on which alkaline phosphatase substrate is used[25-28]. As each substrate has its own optimum reaction conditions, particularly pH, the color reaction procedure must be modified to suit each of them. In the above protocol, we describe conditions for the use of the substrates NBT and BCIP, which are very stable, and in our hands give optimum results. If the hybridization signal, i.e. the colored alkaline phosphatase reaction product, is still weak after an overnight incubation, presumably due to a low content of cellular target mRNA, the color development can be continued for at least another 72 h. Even after 72 h incubation in substrate solution, the background is still very low as long as the washing conditions were sufficiently stringent. While the increase in background is very slow, the specific mRNA signal can increase in strength over a few days. If longer incubation times are necessary, we recommend the use of 17% polyvinyl alcohol in the substrate solution. This may minimize the diffusion of reaction product and background problems. However, the low background in this method is presumably due to the stability of the substrate and the effect of blocking the diffusion of reaction product is not dramatic. The fact that HRP-labelled probes are less sensitive than those which carry an alkaline phosphatase reporter molecule is probably due to the instability of the peroxidase enzyme and its tendency to oxidize and loose activity. In our hands, the alkaline phosphatase reaction products are stable for at least a year when stored out of direct light.

4.3. Cellular localization of the reaction products

Alkaline phosphatase reaction products are, as expected, concentrated in the cell cytoplasm. Sometimes in heavily labelled cells the reaction product is found extending out into the proximal dendrites of neurons. The amount of signal found in the nucleus is usually very low (Fig. 4). The reaction product within the cytoplasm is often seen as punctate clusters, presumably corresponding to groups of polysomes in the endoplasmic reticulum. The subcellular localization of the mRNA signal is most clearly observed in cultured neuronal cells. In these cells, the punctate reaction product is often observed in the cytoplasm close to the nuclear membrane (Fig. 8b,c). This localization of mRNA signal would probably correspond to the sites where rough endoplasmic reticulum (rER) is found. Presumably mRNA is concentrated in this area to facilitate the translation of protein/peptide from mRNA. The position of reaction products is therefore as expected and represents a much higher resolution of signal than can be detected by conventional radioactive probes even with the use of ^{3}H, when the radioactive signal can spread 2–3 μm from its origin. The demonstration of mRNA in primary dendrites also indicates that mRNA actually exists there, and suggests that protein synthesis may occur in them (Fig. 4).

In addition to this unequalled cellular resolution, the background signal is excellent. This is one of the major reasons why the present non-radioactive method has such a high sensitivity (Fig. 5).

Since the detection of the alkaline-phosphatase-linked probe seems comparable or better than radioactive probes, it would seem that problems of penetration of such a large probe into the tissue section do not arise. Treatment of sections with a proteinase digestion to enhance probe penetration has not been found necessary.

4.4. Comparison with the radioactive method

Figure 6 shows an example of the direct comparison between a radioactive in situ hybridization method and the alkaline phosphatase method using either a radiolabelled or an enzyme-labelled somatostatin antisense oligonucleotide probe on adjacent serial sec-

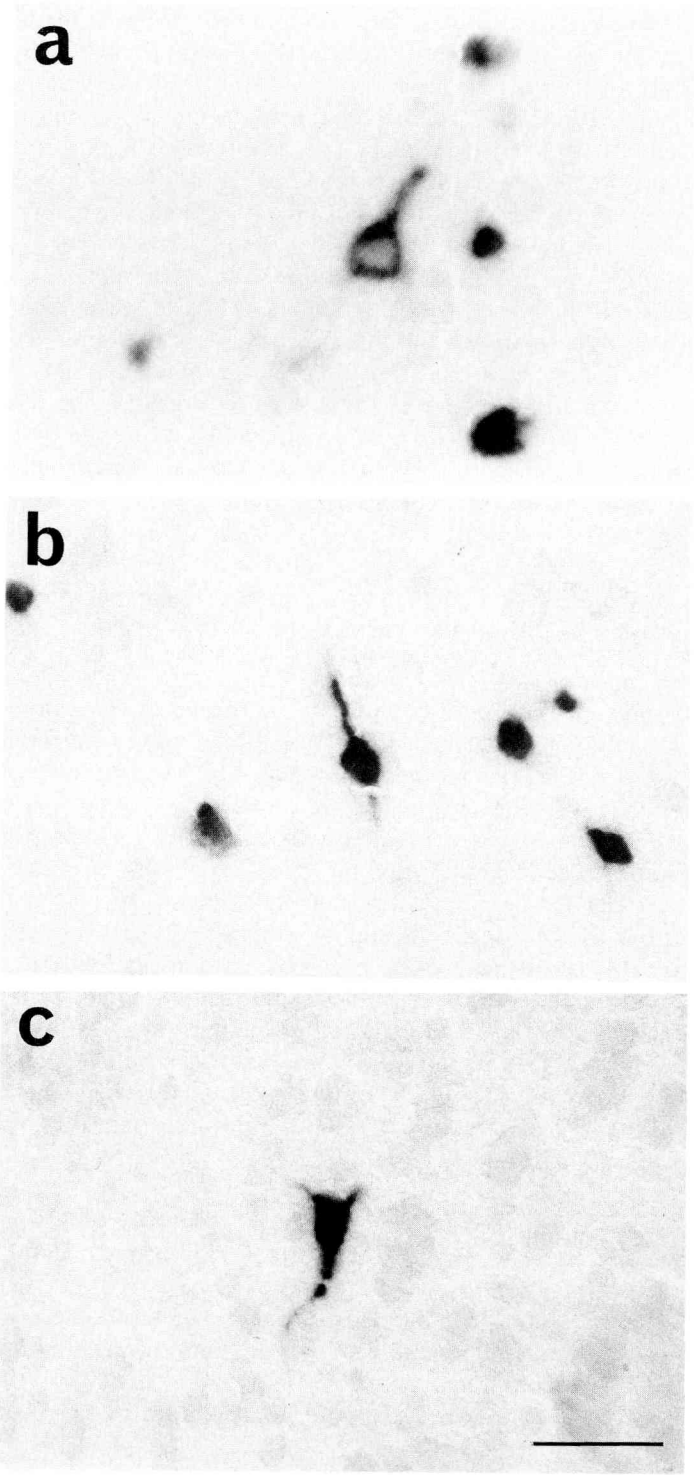

Fig. 4. In situ hybridization histochemistry demonstrated by an alkaline-phosphatase-linked probe. High magnification of a microphotograph demonstrating preprosomatostatin mRNA in rat brain tissue. The mRNA signal is not evenly distributed throughout the cell cytoplasm and some punctate structures are observed. No signal is seen in the nucleus. Punctate mRNA signal is also observed in dendrites. Scale bar = 30 μm.

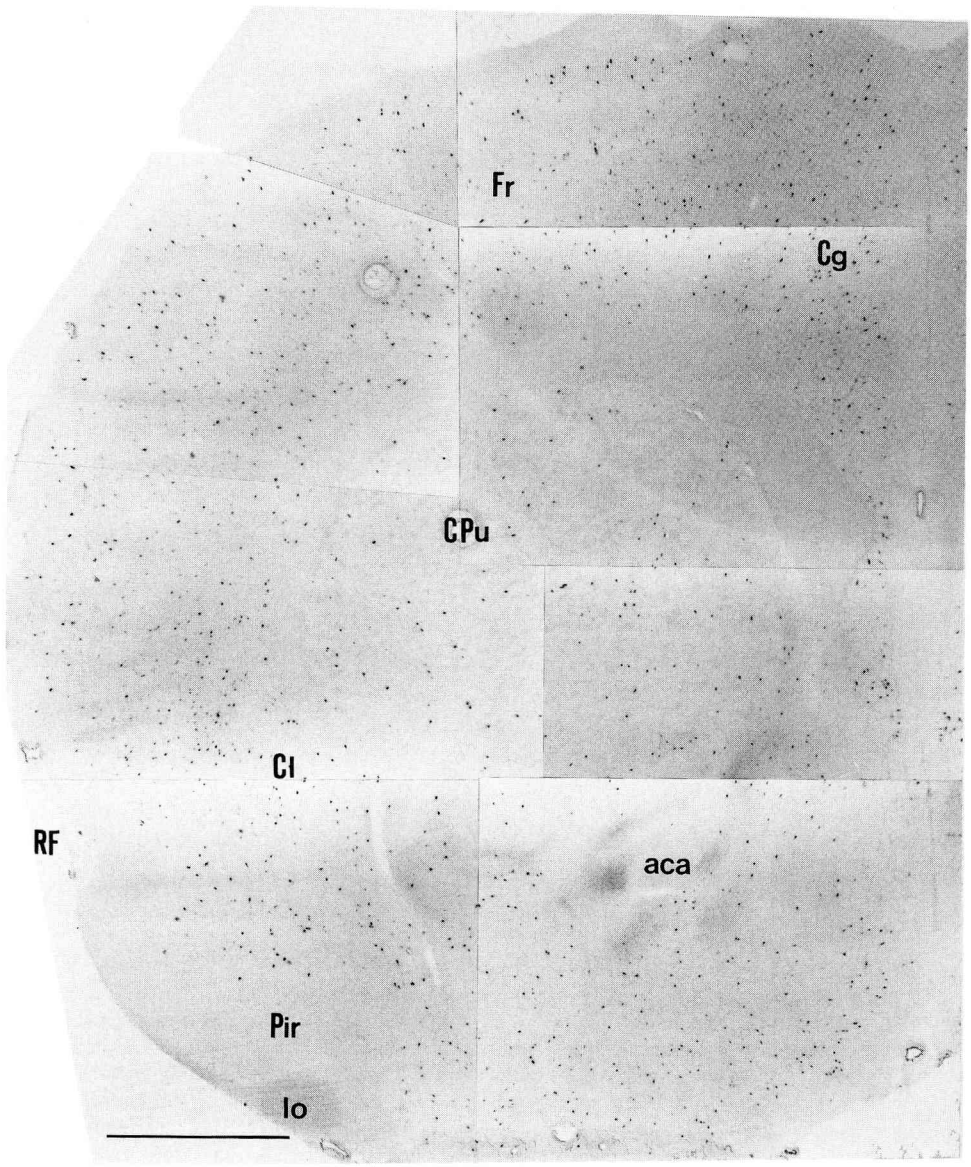

Fig. 5. Photo montage showing the distribution of preprosomatostatin mRNA positive neurons in rat telencephalon using an alkaline phosphatase linked probe. This figure clearly shows how the resolution and contrast between signal and background are excellent. The identification of positive or negative cells is much more obvious than with radioactive in situ hybridization. aca = anterior commissure anterior; Cg = cingulate cortex; Cl = claustrum; CPu = caudate putamen; Fr = frontal cortex; lo = lateral olfactory tract; Pir = piriform cortex; RF = rhinal fissure. Scale bar = 1 mm.

tions. For comparison, in order to achieve the results illustrated it took a week's exposure of the autoradiography film (Fig. 6a), 2 weeks' exposure of the sections for emulsion autoradiography (Fig. 6b,c), but only 1 night to complete the alkaline phosphatase color reaction (Fig. 6d-f). This non-radioactive method is quicker, and any problems with the hybridization reaction or detection of the signal can be rapidly corrected.

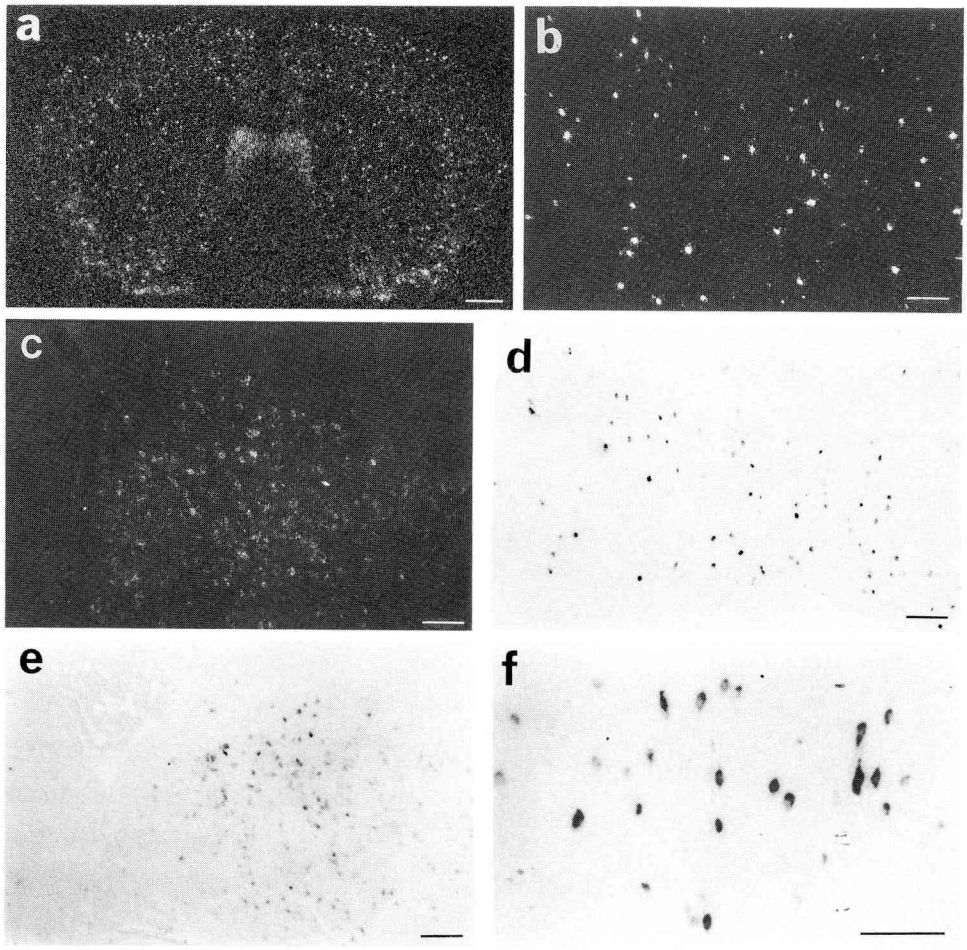

Fig. 6. Comparison between radioactive and non-radioactive probes. Serial sections (15 μm) are prepared for the detection of somatostatin mRNA in the brain using an ^{35}S-labelled probe and an alkaline-phosphatase-labelled probe. (a) Film-autoradiogram using high-resolution, sensitive autoradiography film (2 weeks exposure with Hyper film beta-Max, Amersham, U.K.). (b,c) Emulsion-autoradiograms demonstrated by dark-field illumination (3 weeks exposure with Ilford K-5 nuclear tract emulsion, Ilford, U.K.). (d–f) Non-radioactive in situ hybridization (one overnight color reaction). (b), (d) and (f) demonstrate the mRNA distribution in frontal cortex, and (c) and (e) show the dorsal part of lateral septum. Note that the sensitivity of non-radioactive reaction is comparable to that of radioactive detection with emulsion autoradiography. The individual cells are much more clearly identifiable with the non-radioactive method, particularly in the area like the dorsal part of lateral septum where many positive cells are densely packed together. The positive cells which have low or weak hybridization signal are easier to discern using the non-radioactive probe. Scale bar: a = 1 mm, b–e = 120 μm, f = 100 μm.

The distribution of somatostatin mRNA-positive cells detected by the ^{35}S-labelled probe (autoradiographical silver grains) or alkaline phosphatase color reaction are very similar. However, the cells which are weakly labelled with alkaline phosphatase (i.e. contain a low mRNA content) are much easier to visualize than those cells which contain a low number of silver grains. The reason is that the signal/noise ratio (i.e. the positive signal intensity vs background intensity) is much higher with the alkaline phosphatase method than with the radioactive method. Moreover, in an area where many positive cells

are packed together (cf. Fig. 6a,c,e), the detection of individual positive cells by emulsion autoradiography is often difficult because of the lower resolution of signal due to the spread of the radioactivity through the autoradiography emulsion. With the non-radioactive method, individual positive cells can be clearly detected.

In conclusion, the sensitivity of this non-radioactive in situ hybridization method seems to be comparable to that of the best radioactive methods, at the very least. By comparison, other indirect non-radioactive in situ methods have never achieved this degree of sensitivity.

4.5. Applications to other nervous tissues

4.5.1. Peripheral nerves In peripheral nerves, we found that this method of non-radioactive in situ hybridization was much more effective than the conventional methods using radioactive probes, because individual cells within ganglia could be readily visualized. For example, in autonomic ganglia which consist of rather homogeneous groups of cells which are closely packed, the boundary of each individual cell is rather difficult to detect by autoradiography because of the spread of silver grains. However, with the non-radioactive method, individual separate cells are very clearly detected (Fig. 7a). Another characteristic of peripheral tissues is that they are stratified and follicular. The edges of layers and follicles tend to result in a very high non-specific binding of radiolabelled probes, sometimes called the 'edge effect' in emulsion autoradiography. One reason for this effect may be that the emulsion is thicker at the edge of tissue relative to the rest of the section. This is particularly noticeable in sections from intestinal tissue, which consists of many layers. All of these boundaries, and particularly the submucous layer, may show this 'edge effect'. However, this novel non-radioactive method does not suffer from this problem (Fig. 7b).

Retinal tissue, which again consists of many layers, presents another problem as the cells are packed tightly into nuclear layers making the gaps between cells, and the boundaries of each cell difficult to discern. In this case, a high-resolution signal within the retina was readily obtained using our non-radioactive in situ hybridization method (Fig. 7c).

4.5.2. Neurons in tissue culture Our current method works well on cells grown in vitro. The sensitivity seems comparable to that seen in frozen tissue sections. No problems of penetration of the enzyme-labelled probes were observed, and so far we see no need for proteinase digestion to enhance penetration. Interestingly the resolution at the subcellular level was much better than that observed with tissue sections (Fig. 8), perhaps reflecting the fact that the cell cytoplasm was not damaged by sectioning.

4.5.3. Human tissue The use of in situ hybridization techniques on human tissue is likely to increase, especially when used to investigate pathological gene expression. For diagnostic purposes, a quick and simple method is essential. For this reason, the radioactive method is not ideally suited because of the time scale involved in detecting a signal, and other non-radioactive methods suffer from lack of simplicity and sensitivity. The alkaline phosphatase system described here seems to be among the most suitable so far developed for pathological studies (Fig. 9).

For a postmortem or biopsy tissue sample, the retention of an intact mRNA in the tissue is one of the most important factors in getting a good hybridization signal. Tissue samples must be processed as quickly as possible and the time from collection to freezing or fixing must be minimized.

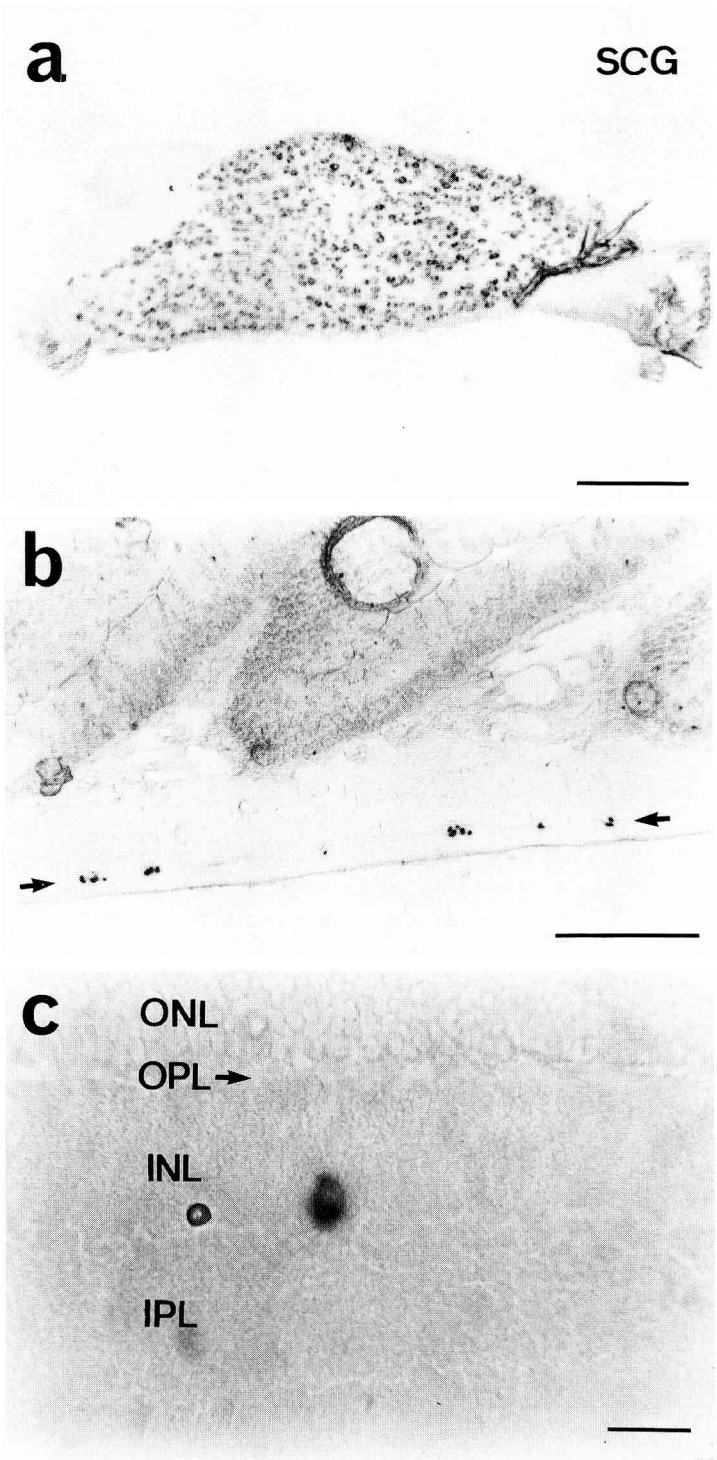

Fig. 7. In situ hybridization with an alkaline-phosphatase-labelled probe in peripheral nervous tissue. (a) Tyrosine-hydroxylase-mRNA-positive cells in rat superior cervical ganglia (SCG). (b) Somatostatin-mRNA-positive myenteric plexus neurons in rat colon. The arrows show the positive cells in myenteric plexus. (c) Somatostatin-mRNA-positive interplexiform cell in rat retina. INL = inner nuclear layer; IPL = inner plexiform layer; ONL = outer nuclear layer; OPL = outer plexiform layer (arrow). Scale bar: a = 200 μm; b = 500 μm; c = 30 μm.

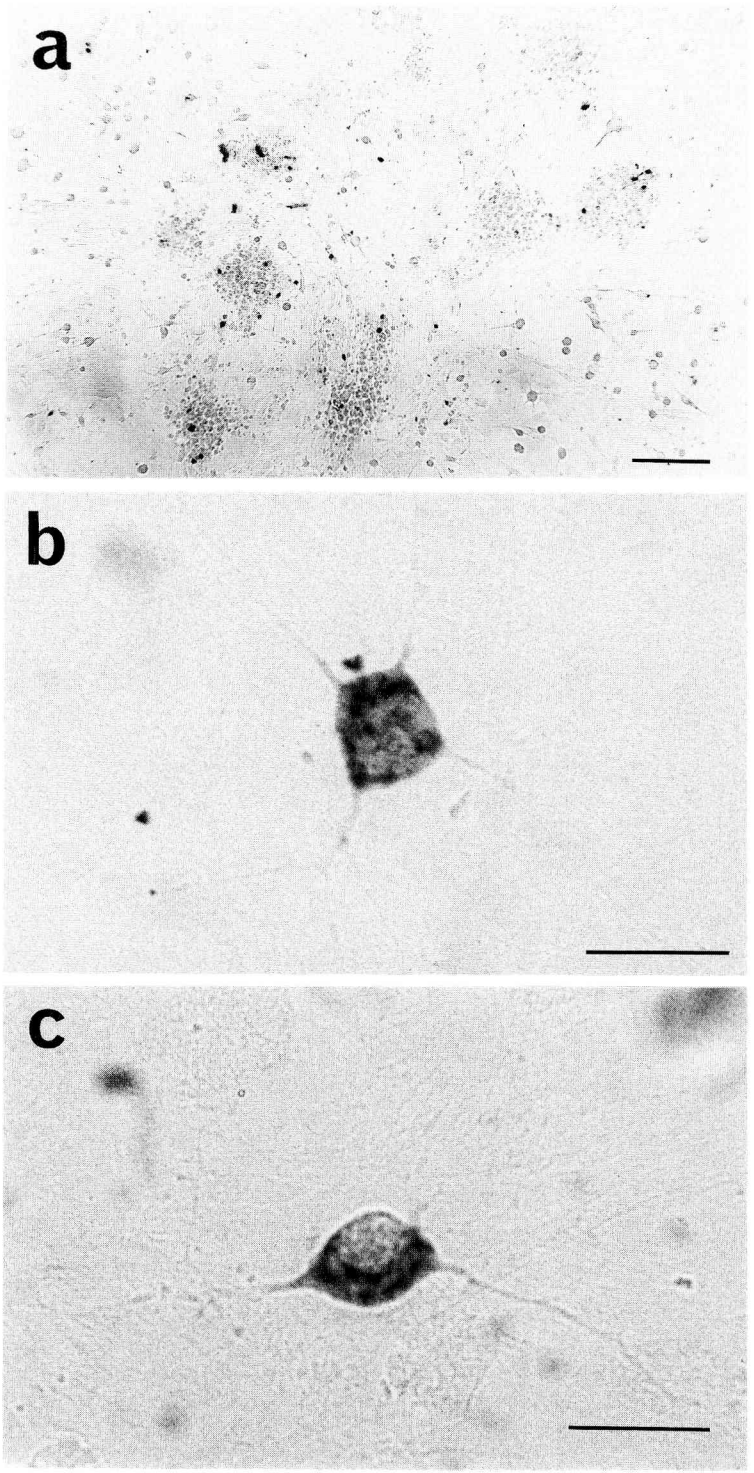

Fig. 8. In situ hybridization on neuronal cell cultures. Cerebral cortical cells from rat embryos were cultured for 2 weeks. An alkaline-phosphatase-labelled somatostatin probe was used. The somatostatin-mRNA-positive reaction product is shown with very high resolution and contrast (a); subcellular localization of mRNA positive signals are observed clearly in each cell at higher magnification (b,c). Punctate positive structures were mainly concentrated in the perinuclear of the cell cytoplasm. Scale bar: a = 100 μm; b,c = 25 μm.

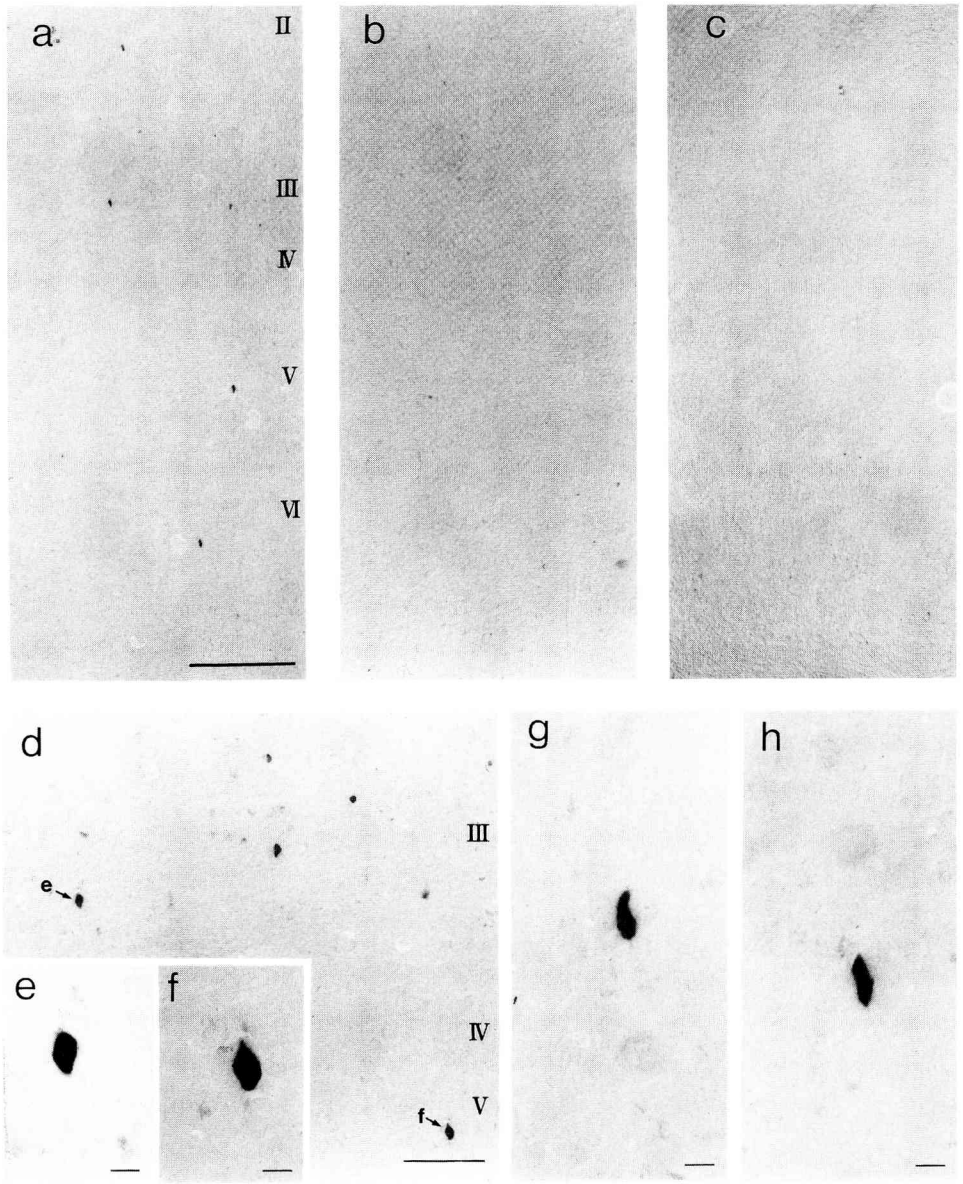

Fig. 9. Human tissue. These photomicrographs show the localization of preprosomatostatin mRNA-positive neurons in human cerebral cortex. The morphology of the positive cell is similar to that seen by immunohistochemistry using somatostatin antisera (a,d–h). (b) and (c) are examples of control experiments in which RNAse pretreatment (b) and competition with excess unlabelled probe (c) were performed. Note that no positive signal is seen in (b) and (c). These experiments were performed using a probe which is a complementary to rat somatostatin mRNA. In this case, no positive signal could be demonstrated using the ordinary hybridization conditions, but could be demonstrated by changing the hybridization buffer composition. This is because there are two base pair mismatches in the probe sequences between human and rat. Scale bar a–c = 400 μm; d = 150 μm; e–h = 20 μm.

4.6. Quantification

As described above, the alkaline phosphatase in situ hybridization method depends on a 1 : 1 reaction of probe with mRNA. Also the signal detection is 'direct' without any

amplification stages and is of a sensitivity equivalent to the best radioactive methods. All these characteristics mean that the strength of signal detected may be directly related to the amount of mRNA present, and that as long as the amount of substrate used does not exceed 10% of the total substrate available the enzyme reaction will not deviate from linearity.

In principle, the relative signal density of individual cells can be measured under equivalent reaction conditions. The difference in relative density correlates well with the observed difference in mRNA content. A microdensitometer, or other image analyzer which can measure the signal intensity of individual cells, is ideal for the relative quantification of the alkaline phosphatase signal[26,59]. In our experience, the change in relative intensity (i.e. mRNA signal) after various chemical treatments corresponds well with data from Northern analysis[26]. The advantage of this 'cellular quantification' over Northern analysis, of course, is the preciseness of signal location, which means that any differences in mRNA expression among cell species and within an area can be detected. In Northern analysis a large tissue sample is homogenized, so any mRNA signal observed is an average of all the cells in that one area.

4.7. Simultaneous visualization of two mRNAs

The improvements described here in the sensitivity of non-radioactive in situ hybridization histochemical methods for detection of mRNA now make it possible to combine non-radioactive and radioactive techniques to visualize two mRNAs on the same section (i.e. to carry out studies of 'co-expression'). So far, a few trials attempting simultaneous visualization of two mRNAs in a section have been carried out, with various combinations of non-radioactive methods, or a mixture of radioactive and non-radioactive methods[20,25,38]. However, earlier successful co-expression studies have been restricted to situations where mRNAs are abundant because of the low sensitivity of earlier non-radioactive probes. Since both the alkaline phosphatase labelled and radioactive probes are among the most sensitive probes so far developed, we have tried to combine them for co-expression studies. After a number of trials our experiments suggest that the use of combinations of short oligodeoxynucleotide probes gives the best results, probably because hybridization and washing conditions can be adjusted so that both radioactive and non-radioactive labelled probes are washed to similar stringency and the probes can be used at equivalent molar concentrations[11,25,28]. The detection of the alkaline phosphatase signal does not influence subsequent autoradiographic detection of labelled cells (Fig. 10).

Both radioactive and alkaline-phosphatase-labelled probes are added to the hybridization buffer at the same time and processed as described earlier. The color reaction is completed first and then the sections are coated with autoradiographic emulsion.

This simultaneous visualization of two mRNAs provides some very interesting results which should extend and hopefully confirm previous immunohistochemical co-localization or co-existence studies.

5. CONCLUSIONS

The development of enzyme-labelled probes has enabled the technique of non-radioactive in situ hybridization to be extended to a level of sensitivity equivalent to the best radioactive methods. The technique described in detail here has a number of advantages including: (a) the reaction can be completed in a few days; (b) a very high signal/noise ratio can be achieved;(c) the signal shows high cellular resolution; (d) the mRNA-positive

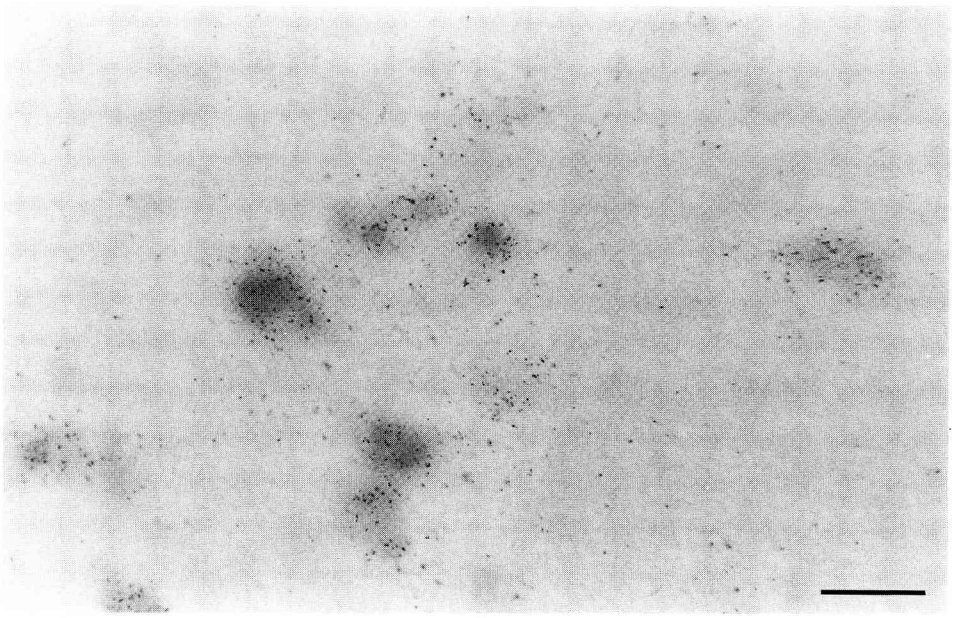

Fig. 10. Simultaneous visualization of two mRNAs in a single section. The tyrosine hydroxylase probe is labelled with alkaline phosphatase and the cholecystokinin (CCK) probe is labelled with a radioisotope. Tyrosine hydroxylase mRNA is visualized by the presence of the alkaline phosphatase colored reaction product. CCK mRNA is visualized by emulsion autoradiography (silver grains). In the rat ventral mescencephalon, double labelled cells, which have both alkaline phosphatase colored reaction product and autoradiographic silver grains, are clearly observed. Scale bar = 30 μm.

cells are readily identified because of their high contrast; (e) the method is very sensitive; (f) it is suitable for semiquantitative analysis; (g) it is well suited to studies of 'co-expression' (where more than one mRNA can be visualized simultaneously); and perhaps most importantly, (h) the method does not require the use of radioactivity with all its attendant hazards and risks to health.

ACKNOWLEDGEMENTS

H. Kiyama acknowledges the support of the Uehara Memorial Foundation (1988), the Japan Society for Promotion of Science (1989) and the Association to Combat Huntington Disease (U.K.). P.C. Emson is a senior member of the MRC staff (U.K.). We are grateful to Drs. D.J. Nunez and S.J. Augood for reading and correcting the manuscript. We are especially grateful to our colleagues Dr. J. Ruth (Molecular Biosystem, San Diego, U.S.A.) and Dr. M. Gait (MRC Laboratory of Molecular Biology, Cambridge, U.K.) for their help in developing the described in situ procedures.

REFERENCES

1 Agrawal, S., Christodoulou, C. and Gait, M.J., Efficient methods for attaching non-radioactive labels to 5′ ends of synthetic oligodeoxyribonucleotides, *Nucleic Acids Res.*, 14 (1986) 6227–6245.

2 Arai, H., Emson, P.C., Agrawal, S., Christodoulou, C. and Gait, M.J., In situ hybridization histochemistry: localization of vasopressin mRNA in rat brain using a biotinylated oligonucleotide probe, *Mol. Brain Res.*, 4 (1988) 63–69.

3 Baldino, Jr., F., Robbins, E., Grega, D., Meyers, S.L., Springer, J.E. and Lewis, M.E., Non-radioactive detection of NGF-receptor mRNA with digoxigenin-dUTP labelled RNA probes, *Soc. Neurosci. Abstr.*, 15 (1989) 345.1.

4 Bauman, J.G.J., Wiegant, J., Borst, P. and Van Duijn, P., A new method for fluorescence microscopical localization of specific DNA sequences by in situ hybridization of fluorochrome labeled RNA, *Exp. Cell. Res.*, 138 (1980) 485–490.

5 Bresser, J. and Evinger-Hodges, M.J., Comparison and optimization of in situ hybridization procedure yielding rapid sensitive mRNA detections, *Gene Anal. Techn.*, 4 (1987) 89–104.

6 Chu, E.C.F. and Orgel, L.E., Ligation of oligonucleotides to nucleic acids or protein via disulfide bonds, *Nucleic Acids Res.*, 16 (1988) 3671–3691.

7 Cremers, A.F.M., Jansen in de Wal, N., Wiegant, J., Dirks, R.W., Weisbeek, P., Van der Ploeg, M. and Lardegent, J.E., Non-radioactive in situ hybridization: a comparison of several immunohistochemical detection systems using reflection contrast and electron microscopy, *Histochemistry*, 86 (1987) 609.

8 Dale, R.M.K. and Ward, D.C., Mercurated polynucleotides: new probes for hybridization and selective polymer fractionation, *Biochemistry*, 14 (1975) 2458–2469.

9 De Jong, A.S.H., Van Kessel-Van Vark, M. and Raap, A.K., Sensitivity of various visualization methods for peroxidase and alkaline phosphatase activity in immunoenzyme histochemistry, *Histochem. J.*, 17 (1985) 1119–1130.

10 Dirks, R.W., Raap, A.K., Van Minnen, J., Vreugdenhil, E., Smith, A.B. and Van der Ploeg, M., Detection of mRNA nucleotides coding for neuropeptide hormones of the pond snail *Lymnaea stagnalis* by radioactive and nonradioactive in situ hybridization: a model study for mRNA detection, *J. Histochem. Cytochem.*, 37 (1989) 7–14.

11 Emson, P.C., Kiyama, H., Ruth, J. and Gait, M., Neuropeptide gene expression: studies of co-expression, *Eur. J. Neurosci.*, Suppl. 2 (1989) 23.8.

12 Foster, A.C., McInnes, J.L., Skingle, D.C. and Symons, R.H., Non-radioactive hybridization probes prepared by chemical labeling of DNA and RNA with a novel reagent photobiotin, *Nucleic Acids Res.* 13 (1985) 745–761.

13 Guitteny, A.-F., Fouque, B., Mougin, C., Teoule, R. and Block B., Histological detection of messenger RNAs with biotinylated synthetic oligonucleotide probe, *J. Histochem. Cytochem.*, 36 (1988) 563–571.

14 Grega, D.S., Cavanagh, T.J., Grimme, S., Martin, R., Lewis, M., Robbins, E. and Baldino, Jr., F., Localization of neuronal mRNA by in situ hybridization using a non-radioactive detection method, *Soc. Neurosci. Abstr.*, 15 (1989) 298.3.

15 Haralambidis, J., Chai, M. and Treger, G.W., Preparation of base-modified nucleotides suitable for non-radioactive label attachment and their incorporation into synthetic oligodeoxy ribonucleotides, *Nucleic Acids Res.*, 15 (1987) 4857–4876.

16 Heiles, B.J., Genersch, E., Kessler, C., Neumann, R. and Eggers, H.J., In situ hybridization with digoxigenin-labeled DNA of human papillomaviruses (HPV 16/18) on HeLa and SiHa cells, *Biotechnique*, 6 (1988) 978–981.

17 Hopman, A.H.N., Wiegant, J. and Van Duijn P., A new hybridocytochemical method based on mercurated nucleic acid probes and sulfhydryl-hapten ligands. II. Effects of variation on the in-situ detection of mercurated probes, *Histochemistry*, 84 (1985) 179–185.

18 Hopman, A.H.N., Wiegant, J. and Van Duijn, P., Mercurated nucleic acid probes: a new principle for non-radioactive in situ hybridization, *Exp. Cell Res.*, 169 (1987) 357–368.

19 Hopman, A.H.N., Wiegant, J., Tesser, G.I. and Van Duijn, P., A non-radioactive in situ hybridization method based on mercurated nucleic acid probes and sulfhydryl-hapten ligands, *Nucleic Acids. Res.*, 14 (1986) 6471–6488.

20 Ichimiya, Y., Emson, P.C., Christodolou, C., Gait, M.J. and Ruth, J.L., Simultaneous visualization of vasopressin and oxytocin mRNA containing neurons in the hypothalamus using non-radioactive in situ hybridization histochemistry, *J. Neuroendocrinol.*, 1 (1989) 73–75.

21 Jablonsky, E., Moomaw, E.W., Tullis, R.H. and Ruth, J., Preparation of oligodeoxynucleotide alkaline phosphatase conjugates and their use as hybridization probe, *Nucleic Acids Res.*, 14 (1986) 6115–6128.

22 John, H., Birnstiel, M. and Tones, K., RNA.DNA hybrids at the cytological level, *Nature*, 223 (1969) 582–587.

23 Keller, G.H., Cumming, C.U., Huang, D.P., Manak, M.M. and Ting, R., A chemical method for introducing haptens onto DNA probes, *Anal. Biochem.*, 170 (1988) 441–450.

24 Keller, G.H., Huang, D.P. and Manak, M.M. Labelling of DNA probes with a photoactivatable hapten, *Anal. Biochem.*, 177 (1989) 392–395.

25 Kiyama, H. and Emson, P.C., Evidence for the co-expression of oxytocin and vasopressin mRNAs in

magnocellular neurosecretary cells: simultaneous demonstration of two neurohypophysin mRNAs by hybridization histochemistry, *J. Neuroendocrinol.*, 2 (1990) 257–259.

26 Kiyama, H., Emson, P.C., Ruth, J. and Morgan, C., Sensitive non-radioactive in situ hybridization histochemistry: demonstration of tyrosine hydroxylase gene expression in rat brain and adrenal, *Mol. Brain Res.*, 7 (1990) 213–219.

27 Kiyama, H., Emson, P.C. and Ruth, J., Distribution of tyrosine hydroxylase mRNA in the rat central nervous system visualized by alkaline phosphatase in situ hybridization histochemistry, *Eur. J. Neurosci.*, 2 (1990) 512–524.

28 Kiyama, H., McGowan, E.M. and Emson, P.C., Co-expression of cholecystokinin mRNA and tyrosine hydroxylase mRNA in population of rat substantia nigra cells: a study using a combined radioactive and non-radioactive in situ hybridization histochemistry, *Mol. Brain Res.* (1990) in press.

29 Kiyama, H., Ruth, J. and Emson, P.C., The detection of somatostatin gene expression by non-radioisotopic in situ hybridization histochemistry, *Eur. J. Neurosci.*, Suppl. 2 (1989) 63.10.

30 Landegent, J.E., Jansen in de Wal, N., Baan, R.A., Hoeijmakers, J.H.J. and Van der Ploeg, M., 2-Acetylamino fluoren modified probes for the indirect hybridocytochemical detection of specific nucleic acids sequence, *Exp. Cell Res.*, 153 (1984) 61–72.

31 Landegent, J.E., Jansen in de Wal, N., Ommen, G.J.B., Baas, F., De Vijlder, J.J.M., Van Duijn, P. and Van der Ploeg, M., Chromosomal localisation of a unique gene by non-autoradiographic in situ hybridization, *Nature*, 317 (1985) 175–177.

32 Langer, P.R., Waldrop, A.A. and Ward, D.C., Enzymatic synthesis of biotin labelled polynucleotides: novel nucleic acid affinity probes, *Proc. Natl. Acad. Sci. USA*, 78 (1981) 6633–6637.

33 Leary, J.L., Brigati, D.J. and Ward, D.C., Rapid and sensitive colorimetric method for visualizing biotin-labeled DNA probes hybridiztion to DNA or RNA immobilized on nitrocellulose: bio-blots, *Proc. Natl. Acad. Sci. USA*, 80 (1983) 4045–4049.

34 Lebacq, P., Squalli, D., Duchene, M., Pouletty, P. and Joannes, M., A new sensitive non isotopic method using sulfonated probes to detect picogram quantities of specific DNA sequences on blot hybridization, *J. Biophys. Biochem. Method*, 15 (1988) 255.

35 Lewis, F.A., Griffiths, S., Dunnicliff, R. and Wells, M., Sensitive in situ hybridization technique using biotin–streptoavidin polyalkaline phosphatase complex, *J. Clin. Pathol.*, 40 (1987) 163–166.

36 Li, P., Moden, P., Skingle, D.C., Lanser, J.A. and Symons, R.H., Enzyme linked synthetic oligonucleotide probes: non-radioactive detection of *Escherichia coli* in faecal specimens, *Nucleic Acids Res.*, 15 (1987) 5275–5287.

37 Lichter, P., Tang, C.C., Call, K., Hermanson, G., Evans, G.A., Housman, D. and Ward, D.C., High resolution mapping of human chromosome 11 by in situ hybridization with cosmid clones, *Science*, 247 (1990) 64–69.

38 Mohr, E., Bahnsen, U., Kiessling, C. and Richter, D., Expression of the vasopressin and oxytocin genes in rats occurs in mutually exclusive sets of hypothalamic neurons, *FEBS Lett.*, 242 (1988) 144–148.

39 Noguchi, K., Senba, E., Morita, Y., Sato, M. and Tohyama, M., α-CGRP and β-CGRP mRNAs are differentially regulated in the rat spinal cord and dorsal root ganglion, *Mol. Brain Res.*, 7 (1990) 299–304.

40 Perrot-Rechenmann, C., Joannes, M., Squalli, D. and Lebacq, P., Detection of phosphoenolpyruvate and ribulose 1-5-*bis* phosphate carboxylase transcripts in maize leaves by in situ hybridization with sulfonated cDNA probe, *J. Histochem. Cytochem.*, 37 (1989) 423–428.

41 Pinkel, D., Straume, T. and Gray, J.W., Cytogenetic analysis using quantitative high sensitivity fluorescence hybridization, *Proc. Natl. Acad. Sci. USA*, 83 (1986) 2934–2938.

42 Poverenny, A.M., Podgorodnichenko, V.K., Bryksina, L.E., Monastyrskaya, G.S. and Sverdolov, E.D. Immunochemical approaches to DNA structure investigation I, *Mol. Immunol.*, 16 (1979) 313–316.

43 Raap, A.K., Marijnen, J.G.J. and Van der Ploeg, M., Anti-DNA.RNA sera, specificity tests and application in quantitative in situ hybridization, *Histochemistry*, 81 (1984) 517–520.

44 Renz, M., Polynucleotide–histone H1 complexes as probes for blot hybridization, *EMBO J.*, 2 (1983) 817–822.

45 Renz, M. and Kurz C., A colorimetric method for DNA hybridization, *Nucleic Acids Res.*, 12 (1984) 3435–3444.

46 Rudkin, G.T. and Stollar, B.D., High resolution detection of DNA-RNA hybrids in situ by indirect immunofluorescence, *Nature*, 265 (1977) 472–473.

47 Ruth, J., Morgan, C. and Paska, A., Linker arm nucleotide analogs useful in oligonucleotide synthesis, *DNA*, 4 (1985) 93.

48 Shroyer, K.R. and Nakane, P.K., Use of DNP-labelled cDNA in in-situ hybridization, *J. Cell Biol.*, 97 (1983) 377a.

49 Smith, L.M., Fung, S., Hunkapiller, M.W., Hunkapiller, T.J. and Hood, L.E., The synthesis of digonucleotides containing an aliphatic amino group of the 5′ terminus: synthesis of fluorescent DNA primers for use in DNA sequence analysis, *Nucleic Acids Res.* 13 (1985) 2399–2412.

50 Sproat, B.S., Beiier, B. and Rider, P. The synthesis of protected 5′-amino 2′,5′-dideoxyribonucleoside-3′-*O* phosphoramidites: application of 5′-amino oligodeoxyribonucleotides, *Nucleic Acids Res.*, 15 (1987) 6181–6196.

51 Sternberger, L.A., *Immunocytochemistry, 2nd edn.*, John Wiley and Sons, New York, 1979.

52 Steward, O. and Falk, P.M., Protein-synthetic machinery at postsynaptic sites during synaptogenesis: a quantitative study of the association between polyribosomes and developing synapses. *J. Neurosci.*, 6 (1986) 412–423.

53 Sverdlov, E.D., Monastyrskaya, G.S., Guskova, L.I., Levitan, T.L., Sheishenko, V.J. and Bukowsky, E.J., Modification of the cytidine residues with a bisulfite-*O*-methyl hydroxylamine mixture, *Biochim. Biophys. Acta*, 340 (1974) 153.

54 Syvanen, A.-C., Nucleic acid hybridization: from research tool to routine diagnostic method, *Med. Biol.*, 64 (1986) 313–324.

55 Tchen, P., Fuchs, R.P.P., Sage, E. and Leng, M., Chemically modified nucleic acids immunodetectable probes in hybridization experiments, *Proc. Natl. Acad. Sci. USA*, 81 (1984) 3466–3470.

56 Uhl, G.R., *In situ Hybridization in Brain*, Plenum Press, New York, 1986.

57 Urdea, M.S., Warnner, B.D., Running, J.A., Stempien, M., Clyne, J. and Horn, T., A comparison of non-radioisotopic hybridization assay methods using fluorescent, chemiluminescent and enzyme-labelled synthetic oligodeoxyribonucleotide probes, *Nucleic Acids Res.*, 16 (1988) 4937–4956.

58 Valentino, K.L., Eberwine, J.H. and Barchas, D.J., *In situ Hybridization: Application to Neurobiology*, Oxford University Press, Oxford, 1987.

59 Van Noorden, C.J.F. and Jonges, G.N., Quantification of the histochemical reaction for alkaline phosphatase activity using the indoxyl-tetranitro BT method, *Histochem. J.*, 19 (1987) 94–102.

60 Vincent, C., Tchen, P., Cohen-Solal, M. and Kourilsky, P., Synthesis of 8-(2,4-dinitrophenyl-2,6-aminohexyl)amino-adenosine 5′-triphosphate: biological properties and potential uses, *Nucleic Acids Res.*, 10 (1982) 6787–6796.

Neuroscience Vol. 38, No. 1, pp. 223–244, 1990
Printed in Great Britain

主論文 (2)

0306-4522/90 $3.00 + 0.00
Pergamon Press plc
IBRO

DISTRIBUTION OF SOMATOSTATIN mRNA IN THE RAT NERVOUS SYSTEM AS VISUALIZED BY A NOVEL NON-RADIOACTIVE *IN SITU* HYBRIDIZATION HISTOCHEMISTRY PROCEDURE

H. KIYAMA* and P. C. EMSON

MRC Group, AFRC Institute of Animal Physiology and Genetics Research, Babraham, Cambridge CB2 4AT, U.K.

Abstract—The cellular localization of preprosomatostatin mRNA in the rat brain and sensory ganglia has been examined in detail using a newly developed highly sensitive non-radioactive *in situ* hybridization histochemistry procedure. An alkaline phosphatase labelled anti-sense 30mer oligodeoxynucleotide probe was used for detection of somatostatin mRNA. This probe readily demonstrated somatostatin gene expression throughout the rat CNS with very high contrast and good cellular localization. As a result, we visualized numerous somatostatin mRNA-positive cells in many CNS areas which had previously not been shown to contain a mRNA signal. This method detected a number of somatostatin mRNA-positive cells, in the mitral cell layer of accessory olfactory bulb, the glomerular layer of the main olfactory bulb, the dorsal part of the lateral septum, superficial gray layer of superior colliculus, inferior colliculus, anterior ventral cochlear nucleus, granular layer and Purkinje cell layer of cerebellum, and substantia gelatinosa of medulla and spinal cord, all areas where signal detection using radiolabelled *in situ* probes has previously been rather difficult.

The principle advantages of the present method include the very precise cellular resolution of signal, the rapid reaction time and low background. The sensitivity of the present method seems to be at least equivalent to most immunocytochemical procedures and more sensitive than most isotopic *in situ* hybridization methods.

Somatostatin, or growth-hormone release inhibiting factor, was first isolated and sequenced from hypothalamic extracts by Brazeau *et al.*[4] The sequencing of the peptide enabled a number of antibodies to be raised to the tetradecapeptide (somatostatin$_{14-28}$) sequence and a number of immunohistochemical studies were carried out to determine the distribution of somatostatin-immunoreactive structures in the CNS.[1,3,5–11,13,17,18,21,23,27–29,35,36,40–42,44–46,50] Subsequently the development of antibodies to other molecular forms of somatostatin (somatostatin$_{1-28}$ or somatostatin$_{1-12}$) extended these studies,[32,33] and most recently the development of molecular cloning techniques has enabled the technique of *in situ* hybridization to be used to demonstrate the presence of somatostatin mRNA in the rat brain using radioactive antisense oligodeoxynucleotide, cDNA or cRNA probes.[12,16,34,39,48]

The technique of *in situ* hybridization using radiolabelled probes is technically complex, requiring facilities for handling or labelling oligonucleotide, cDNA or cRNA probes, and uses autoradiography to detect labelled cells with limited resolution.[47,49] For this reason it would be useful to have non-radioactive *in situ* hybridization techniques which are both sensitive, at least semi-quantitative and capable of excellent resolution of signal within the cell.[2,19,24–26] In this study the use of an enzyme-labelled (alkaline phosphatase) antisense oligodeoxynucleotide probe is described which has been used to visualize sites of somatostatin gene expression in the rat brain.[24–26]

*To whom correspondence should be addressed at: Department of Neuroanatomy, Biomedical Research Center, Osaka University Medical School, 4-3-57 Nakanoshima, Kitaku, Osaka (530), Japan.

Abbreviations: BCIP, 5-bromo-4-chloro-3-indolyl phosphate; DSS, disuccinimidyl suberate; EDTA, ethylenediaminetetra-acetate; NBT, nitroblue tetrazolium; PBS, phosphate-buffered saline; SSC, saline sodium citrate.

EXPERIMENTAL PROCEDURES

Preparation of probe

For detection of somatostatin mRNA an antisense alkaline phosphatase-labelled oligodeoxynucleotide (30mer) was used.[26] The sequence of the probe is complementary to bases 310–339 of the rat preprosomatostatin cDNA, the region of the cDNA coding for somatostatin-14.

Calf intestinal alkaline phosphatase was cross-linked to a single modified base with a 12-atom linker arm which was included during the synthesis of the oligonucleotide. Full experimental details of this procedure are described by Ruth *et al.*[22,38] In brief the modified base replaced a thymidine and was incorporated directly into the automated synthesis carried out on DNA synthesizer (Applied Biosystem Model 380A). Alkaline phosphatase was cross-linked to the primary amine group using disuccinimidyl suberate (DSS). The alkaline phosphatase–oligonucleotide conjugate was separated from the unlabelled oligonucleotide by gel filtration and anion-exchange chromatography.[22]

Tissue preparation

Twelve male Sprague–Dawley rats (200–250 g) were used. Animals were decapitated and the brain and spinal cord

removed together with the dorsal root and trigeminal ganglia. These tissues were quickly frozen on dry ice. Fresh frozen sections were cut (15 μm thickness) using a cryostat (Bright, Huntington, U.K.) and thaw mounted onto chrome–alum coated slides. For control experiments three serial sections were cut; the first section was used for hybridization of the somatostatin oligonucleotide probe, the second section was used for ribonuclease A pretreatment (to digest cellular mRNAs) and the third section for competition experiments with an excess of non-labelled probe. The non-labelled probe contains only the modified base and did not carry the alkaline phosphatase reporter group (Fig. 1). All these sections were kept at −20°C until used.

In situ *hybridization*

Frozen sections were warmed quickly from −20°C to room temperature using a hair drier. Sections were then immediately fixed with 4% paraformaldehyde in 0.1 M phosphate buffer (pH 7.4) for 30 min at room temperature. Fixed sections were then rinsed twice with 0.1 M phosphate-buffered saline (PBS) which had been treated with 0.1% diethylpyrocarbonate and autoclaved before use. Sections were then pretreated with 0.25% acetic anhydride in 0.1 M triethanolamine/0.9% NaCl for 10 min at room temperature. After this pretreatment, the sections were dehydrated through 70, 80, 90, 95% ethanol and absolute ethanol (5 min each), delipidated with chloroform for 10 min, washed with absolute and 95% ethanol for 5 min each, and dried. Dried sections were then hybridized in the following hybridization buffer; 4 × saline sodium citrate (SSC), 50% deionized formamide, 1 × Denhardt's solution, 500 μg/ml sheared salmon testis DNA, and 10% dextran sulphate. The alkaline phosphatase-labelled oligodeoxynucleotide probe was used at a final concentration of 4 fmol/μl. The total volume of hybridization buffer applied to each section was approximately 50 μl. Sections were then hybridized overnight at 37°C in moist chambers. Following hybridization sections were dipped in 1 × SSC to remove the hybridization buffer, washed stringently four times in preheated 1 × SSC at 55°C each for 20 min, and again washed in 1 × SSC for 1 h at room temperature. After these washings, the buffer was changed to 0.1 M Tris–HCl (pH 7.5) containing 0.9% NaCl for 30 min followed by 0.1 M Tris–HCl (pH 9.5) containing 0.1 M NaCl and 0.05 M $MgCl_2$ for 10 min to provide buffer pH and salt concentration appropriate for colour development. The stock alkaline phosphatase substrates nitroblue tetrazolium (NBT; 75 mg/ml) and 5-bromo-4-chloro-3-indolyl phosphate (BCIP; 50 mg/ml) were obtained from Boehringer Mannheim and kept at −20°C until used. Final concentrations of the substrates in the Tris–HCl (pH 9.5) were 340 μg/ml NBT and 170 μg/ml BCIP. Alkaline phosphatase substrate solution was applied to each slide (1 ml) and the slides were kept in dark moist chambers at room temperature overnight. The sections were all developed for the same time (18 h) so that relative comparison between the quantity of mRNA signal might be made between sections hybridized and developed for the same time. Under the incubation conditions used, less than 1% of the available alkaline phosphatase substrate is used so that the enzyme reaction does not deviate from linearity. Colour development was terminated by incubating in 10 mM EDTA in 10 mM Tris–HCl buffer (pH 7.5) for 1 h. Finally, slides were coverslipped using EDTA/Tris–HCl buffer containing 50% glycerol. The alkaline phosphatase signal was stable under these conditions for at least a year.

The specificity of the alkaline phosphatase probe was tested by two types of control experiments. Firstly, pretreatment of sections with RNase A (20 μg/ml) for 30 min at room temperature, which digests cellular mRNA in the tissue sections. RNase A treatment was carried out just prior to hybridization. Sections were then washed with PBS/diethylpyrocarbonate three times, each wash lasting 10 min. These sections were then hybridized in the normal hybridization buffer. This control was also checked to see that the alkaline phosphatase-labelled oligonucleotide was

Abbreviations used in figures

3V	third ventricle
4V	fourth ventricle
aca	anterior commissure anterior
aci	anterior commissure interbulbar
AO	anterior olfactory nucleus
Aq	aquaduct of midbrain
Arc	arcuate nucleus
BM	basomedial amygdaloid nucleus
CA1–3	field CA1–3 of Ammon's horn
cc	corpus callosum
Ce	central amygdaloid nucleus
CNS	central nervous system
CPu	caudate-putamen
cu	cuneate fasciculus
dr	dorsal root
DR	dorsal raphe nucleus
DRG	dorsal root ganglia
ECIC	external cortex of inferior colliculus
EPl	external plexiform layer (olfactory bulb)
GI	glomerular layer (olfactory bulb)
GP	globus pallidus
Gr	granular layer (olfactory bulb)
GrDG	granular layer of dentate gyrus
Grl	granular layer (cerebellum)
IGr	internal granular layer (olfactory bulb)
LH	lateral hypothalamus
lo	lateral olfactory tract
LPB	lateral parabrachial nucleus
LPO	lateral preoptic area
LSD	dorsal subnucleus of lateral septal nucleus
LSI	intermediate part of lateral septal nucleus
LV	lateral ventricle
ME	median eminence
Me	medial amygdaloid nucleus
MG	medial geniculate body
Mi	mitral cell layer (olfactory bulb)
mlf	medial longitudinal fasciculus
Mo	molecular layer of cerebellum
Mol	molecular layer of dentate gyrus
opt	optic tract
Or	oriens layer of hippocampus
ox	optic chiasma
Pa5	paratrigeminal tract nucleus
Par	pariatal cortex
Pe	periventricular nucleus of hypothalamus
Pir	piriform cortex
PoDG	polymorph layer of dentate gyrus
Prh	prepositus hypoglossal nucleus
Puj	Purkinje cell layer
Py	pyramidal layer of hippocampus
pyx	pyramidal decussation
Rad	stratum radiatum (hippocampus)
s5	sensory root of trigeminal nerve
scp	superior cellebellar peduncle
Sol	solitary tract nucleus
Sp5	spinal trigeminal nucleus
Sp5C	spinal trigeminal nucleus caudal
SuG	superficial gray layer of superior colliculus
VCA	ventral cochlear nucleus pars anterior
VLL	ventral nucleus of lateral lemniscus
VM	ventromedial thalamic nucleus
VMH	ventromedial hypothalamic nucleus
ZI	zona incerta

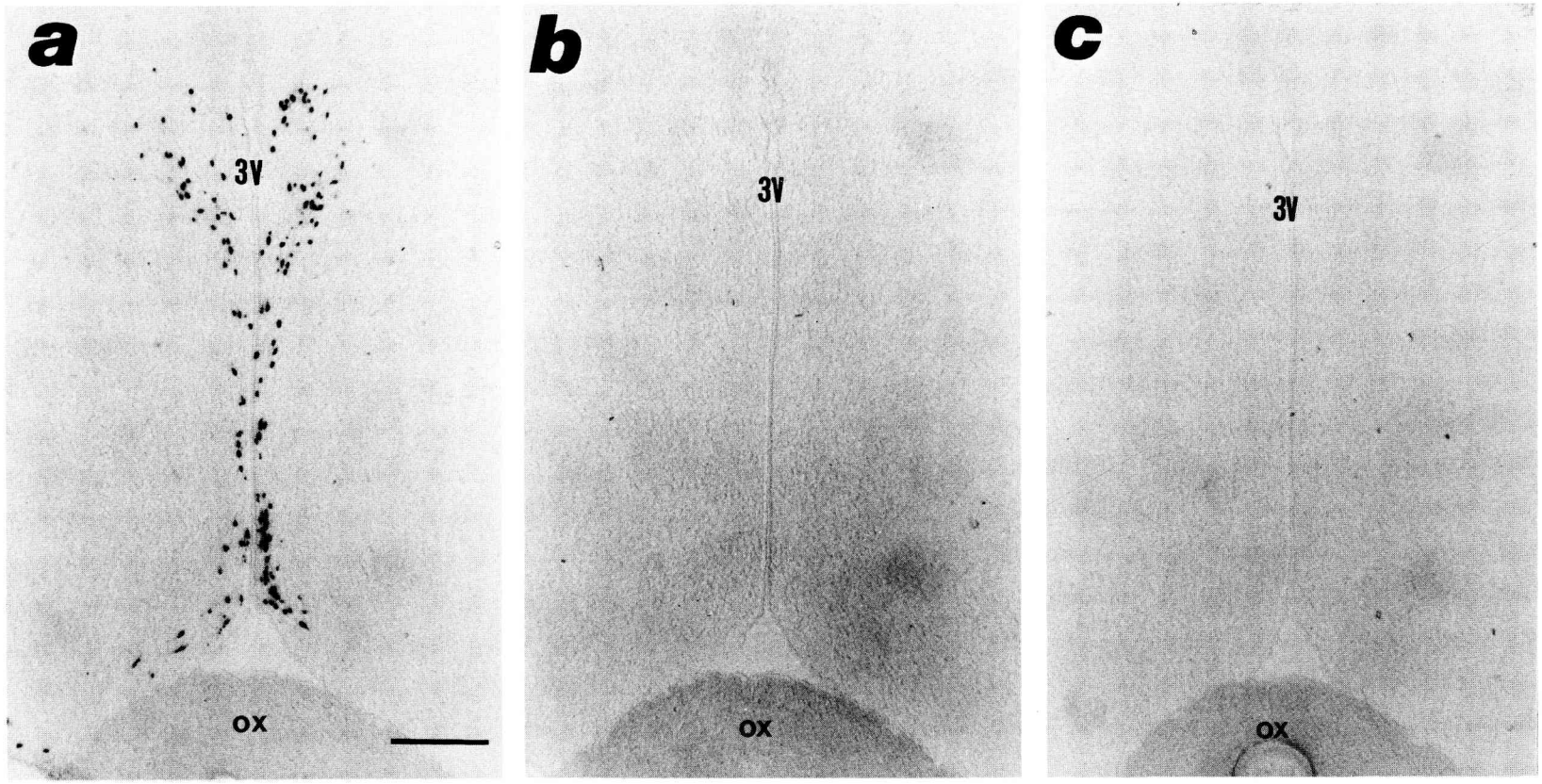

Fig. 1. Histological control experiments. Three serial sections were obtained for control experiments (a–c) from the area containing periventricular nucleus of hypothalamus. (a) Positive control section. (b) RNase A pretreated section. (c) Competition experiment with an excess of non-labelled probe (see Experimental Procedures). Note that no somatostatin mRNA-positive cells were found in any control experiment (b and c). Scale bar = 500 μm.

not binding non-specifically to the tissue sections or the slide. Secondly, tissue sections were incubated with an excess of non-labelled oligonucleotide probe (400 fmol/μl) which had the modified base and the linker arm but did not carry the alkaline phosphatase reporter group. Both alkaline phosphatase-labelled and non-labelled probes were added to the hybridization buffer at the same time. Neither control experiment demonstrated a detectable hybridization signal (Fig. 1).

Densitometry

The relative optical density of the alkaline phosphatase signal was determined using a Vickers Micro Densitometer M85 (Vickers Instrument, U.K.). The machine detected the relative optical density (525 nm) of individual cells. Individual cellular optical density recordings were determined by integrating the optical density in a 2×2 μm area within the cell cytoplasm. At least 20 cells in each area or nucleus were sampled to determine an average signal density per area/or nucleus. Cells were classified as containing very intense, intense, moderate, weak (low) and very weak (very low) signals depending on their average relative optical density value: very intense >30 units, intense 20–30 units, moderate 10–20 units, weak 5–10 units, very weak <5 units. The amount of signal is relative, but to illustrate this point representative cells corresponding to this classification are illustrated in Fig. 2.

RESULTS

Telencephalon

Olfactory bulb. In the glomerular layer and internal granular layer of the main olfactory bulb, a variety of somatostatin mRNA-positive cells were found. Several small cells which had a weak hybridization signal were found in the glomerular layer (Fig. 3a). These cells were thought to be periglomerular cells, due to their round cell profile and anatomical position. A few positive cells per section were also found in the internal granular layer (Fig. 3b). The number of positive cells in the internal granular layer was much less than in the glomerular layer, but the hybridization signal in each cell was distinctly stronger, being moderate to intense. These medium sized cells were thought to be granular cells. A large number of somatostatin mRNA-positive cells were also localized in the anterior olfactory nucleus. These cells were distributed in all the sub-nuclei, lateral, dorsal, medial and ventral nuclei of the anterior olfactory nucleus and were found throughout the rostrocaudal extent of the nucleus (Fig. 3c). The strength of hybridization signal for these cells was intense and equivalent to that found in the strongly positive cerebral cortical cells (see below). In accessory olfactory bulb, the distribution of somatostatin mRNA-positive cells was distinctly different from that seen in the main olfactory bulb. A moderate number of somatostatin mRNA-positive cells (20–30 cells per hemi-section) were observed in the mitral cell layer with a few positive cells also in the granular layer (Fig. 4). Although information as to the dendritic features of these positive cells would be required to classify them unambiguously, these positive cells were presumed to be mitral cells due to their anatomical location and cell size (15–20 μm). The

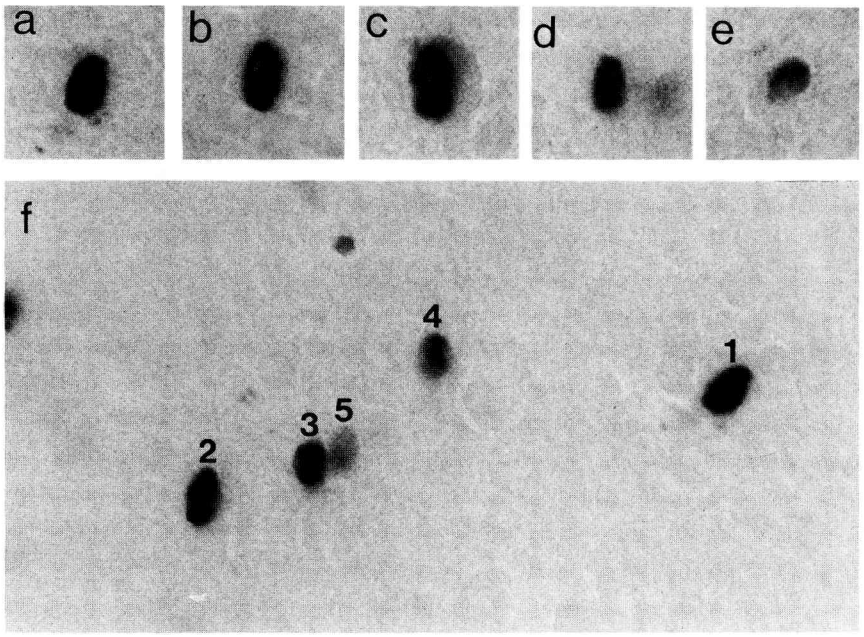

Fig. 2. Examples of the variation in somatostatin mRNA gene expression within an individual section. The relative optical density of the cells (a–e) from cerebral cortex were determined using a Vickers M85 microdensitometer (see Experimental Procedures). The relative optical density of these cells illustrated in (a)–(e) are as follows: (a) 32.752 ± 0.88; (b) 27.80 ± 0.69; (c) 15.60 ± 0.81; (d) 8.74 ± 0.89; (e) 4.16 ± 0.07. We arbitrarily assigned five categories of cell signal (very intense >30 units, intense 20–30 units, moderate 10–20 units, weak 5–10 units, very weak <5 units). (f) Another example of the variation in cellular mRNA signal. These five numbered cells belong to the five categories described above (1, very intense; 2, intense; 3, moderate; 4, weak; 5, very weak).

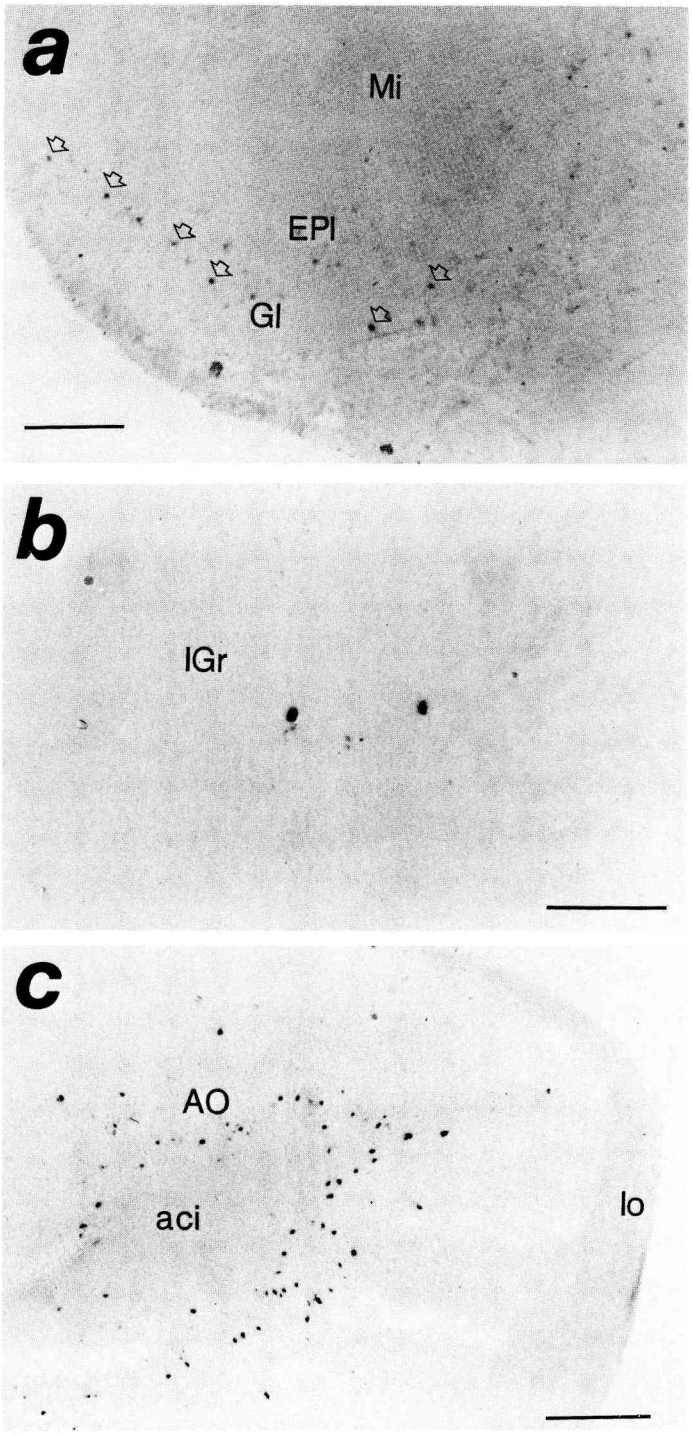

Fig. 3. Somatostatin mRNA-positive cells in olfactory bulb. (a) Somatostatin mRNA-positive cells in glomerular layer (arrows) of the main olfactory bulb. (b) Some intensely stained cells are found in the inner granular layer (IGr). (c) A number of intensely stained somatostatin mRNA-positive cells were found in all parts of anterior olfactory nuclei (AO). Scale bars = 150 μm (a); 200 μm (b); 400 μm (c).

hybridization signal in the mitral cell layer was moderate in some 20–30% of the somatostatin mRNA-positive cells and only weak in the remaining 70–80% of cells. In contrast, the somatostatin mRNA-positive cells in the granular layer contained an intense signal equivalent to the signal strength observed in the granuler layer of the main olfactory bulb.

Cerebral cortex. The cerebral cortex was especially rich in somatostatin mRNA-containing cells. In the neocortex, somatostatin mRNA-positive cells were observed in all layers with the exception of layer I.

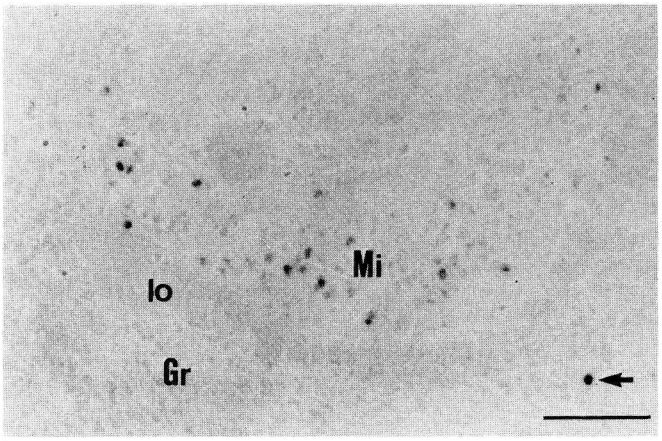

Fig. 4. Somatostatin mRNA-positive cells in the accessory olfactory bulb. Several somatostatin mRNA-positive cells were observed in mitral cell layer (Mi) and a few positive cells were found in the granular layer (arrow). Scale bar = 200 μm.

The distribution of cells among these layers was not even (Fig. 5). The highest density of positive cells was observed in layers V and VI (20–25 cells/0.25 mm^2), the second highest density of positive cells was found in layers II and III (15–20 cells/0.25 mm^2), and the lowest density of positive cells was in layer IV (5–10 cells/0.25 mm^2). In layers II and III, 70–80% of positive cells had a very intense hybridization signal whilst the other 20–30% of positive cells had a moderate or weak signal. These layer II and III cells were round (15–20 μm) or elongated (long axis about 25 μm, short axis about 10 μm) in shape. In contrast, most of the cells found in layer IV had a weak mRNA signal. In the deeper layers, V and VI, the percentage of somatostatin mRNA-positive cells which had an intense signal increased again. Some 40–50% of positive cells in layers V and VI had a very intense signal, whilst the others had a moderate or weak signal. These cells were all medium or small sized (10–20 μm) and usually round. Although the density of positive cells was greatest in the deep layers (V–VI). the percentage of cells having an intense mRNA signal was higher in the surface layers (II–III) than in the deeper layers. A few somatostatin mRNA-positive cells were also found in the corpus callosum (4–7 cells per section), and many of these had elongated soma with fibres running in the corpus callosum. In the cingulate cortex, many somatostatin mRNA-positive cells were also found. The density of positive cells seemed to be similar to the neocortex, with some 20–30% of cells containing an intense mRNA signal, the other 70–80% of positive cells containing only a moderate or weak signal. In the pyriform cortex, somatostatin mRNA-positive cells were found mainly in the deep layer (layer III), and rarely in the pyramidal cell layer (layer II). No somatostatin-positive cells were found in layer I. The cell density in layer III was similar to that found in the neocortex. Only four or five positive cells were found in layer II. The positive cells in both layers II and III were medium or small in size (10–20 μm) and had a very strong mRNA signal. Somatostatin mRNA-positive cells were also found in the endopyriform nucleus and claustrum. These cells had a similar signal density equivalent to that found in the positive cells of layer III of the pyriform cortex, but the cell density was a little less than that found in layer III of the pyriform cortex. In the entorhinal cortex, the number of positive cells was a little less than that found in neocortex. The large cells, which are the main component of layer II of the entorhinal cortex, did not contain any positive signal, but some other small cells (10–15 μm) in this layer contained a positive hybridization signal. In the other layers (layers III–VI) of the entorhinal cortex a moderate number of medium sized cells was found with the exception of layer IV (cell sparse zone), where only a small number of positive cells was found.

Hippocampus. In the hippocampal complex, all areas contained somatostatin mRNA-positive cells. In the CA1, medium to large cells (20–25 μm) were concentrated in the oriens layer (Fig. 6a). Most of these cells had an intense signal (for details see Fig. 6d). Only a few medium sized positive cells were found in the pyramidal layer and only one or two positive cells were found in the stratum radiatum per hemi-section. In the CA2, although a moderate number of positive cells existed in the oriens layer, the number of cells found in the pyramidal layer and stratum radiatum was significantly greater than in CA1. Furthermore, in CA3, the number of positive cells in radiatum exceeded the number in the oriens layer. Positive cells in CA2 and CA3 generally contained less hybridization signal than those in CA1. The areas CA1, CA2 and CA3 had their own distinct distribution pattern of somatostatin mRNA-positive cells and this difference was maintained throughout the rostocaudal extent of the hippocampus. In the dentate gyrus, the number of positive cells and the signal density of each positive cell was similar to that found in CA1

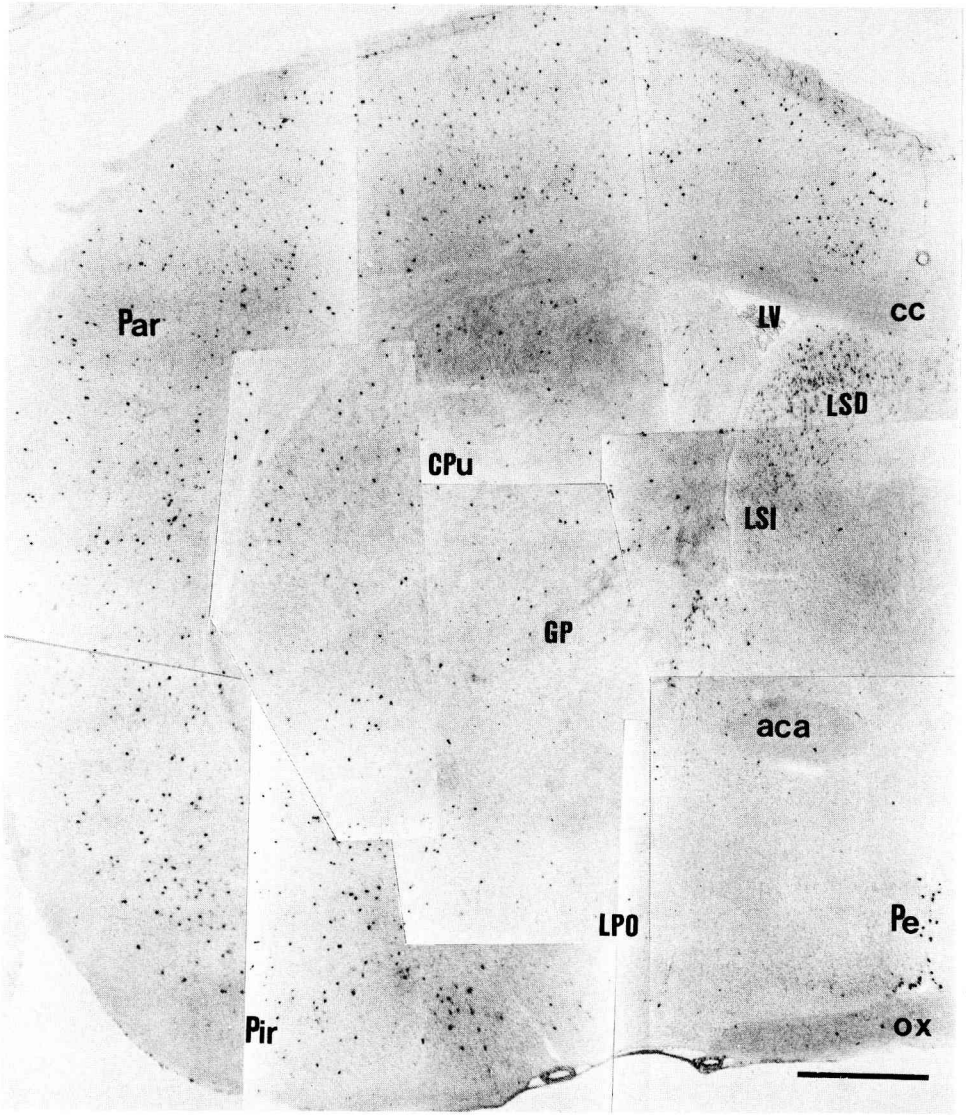

Fig. 5. Montage photomicrograph of the telencephalic region containing cerebral cortex, basal ganglia, septum and anterior part of hypothalamus. Somatostatin mRNA-positive cells were readily visible against a pale background. Large numbers of positive cells were present in the cerebral cortex and dorsal part of lateral septum (LSD). Note the density of hybridization signal differs substantially between cerebral cortical cells (intensely stained) and cells in LSD which typically contained only a weak hybridization signal. Scale bar = 1 mm.

(Fig. 6b,c). The somatostatin mRNA-positive cells were localized only in the polymorph layer of dentate gyrus[37] and were not found in the granular layer or in the inner and outer blade areas. This pattern of distribution of somatostatin mRNA cells was maintained throughout all levels of the dentate gyrus. The subiculum proper, para- and presubiculum contained fewer positive cells (5–10 cells/0.25 mm^2) than Ammon's horn, with most of the subicular cells containing only a weak somatostatin mRNA signal, although a few individual cells contained a moderate amount of signal.

Septum. Numerous medium or small positive cells were found in the dorsal subnucleus of the lateral septum nucleus (approximately 70–90 cells/0.25 mm^2). This represents a much higher cell density than was found in the neocortex (Fig. 5). This high density of cells was seen throughout all levels of the dorsal subnucleus of lateral septal nucleus, although the hybridization signal per individual cell was weak. A few positive cells per section were also observed in the intermediate part of the lateral septa nucleus, although all the cells were located near the dorsal subnucleus of lateral septal nucleus and these cells had a signal strength comparable to the positive cells in the dorsal subnucleus of lateral septal nucleus.

Amygdala. All nuclei in the amygdaloid complex proper contained numerous somatostatin mRNA-positive cells, with some positive cells being found in

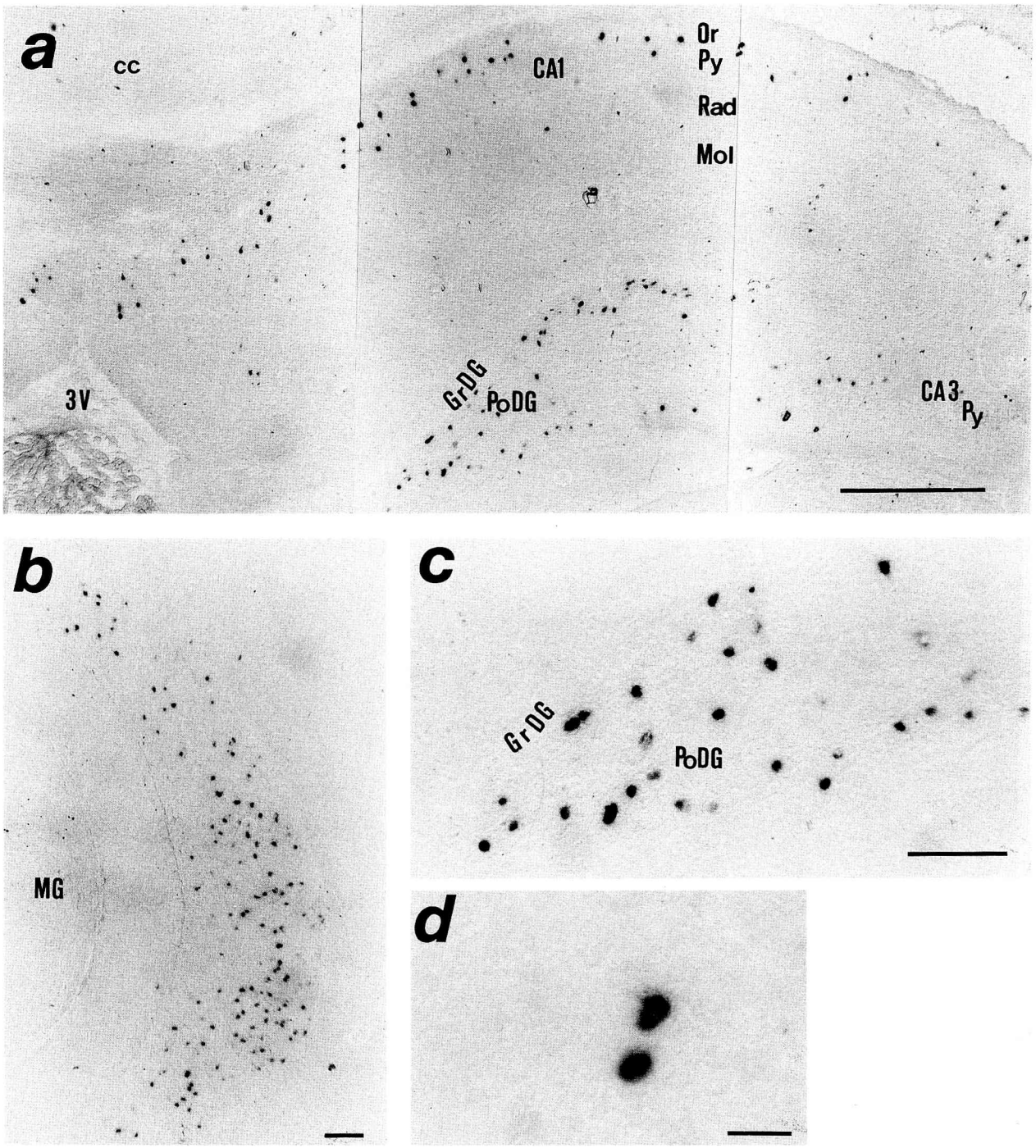

Fig. 6. Somatostatin mRNA-positive cells in hippocampus. (a) Montage photomicrograph showing CA1, 3 and dentate gyrus. (b) Caudal part of dentate gyrus. (c) Higher magnification of dentate gyrus from the same section as illustrated in (a). (d) Higher magnification of somatostatin mRNA-positive cells in stratum oriens of CA1. Note the positive staining is particularly concentrated in cytoplasm of the cell somata. Scale bars = 800 μm (a); 200 μm (b, c); 50 μm (d).

the border area of the amygdala. The central nucleus of the amygdaloid complex contained the highest density of positive cells (Fig. 7a) with about 80–100 positive cells per 0.25 mm^2. Most of these cells were small or medium in size (10–20 μm), round in shape, with a weak to moderate hybridization signal (for details see Fig. 7b). The next highest cell density was found in the medial nucleus (30–40 cells/0.25 mm^2); however, only one third of the positive cells in this nucleus had an intense signal, whilst the remaining positive cells had a weak to moderate mRNA signal. The basal, lateral and cortical nuclei all had a similar

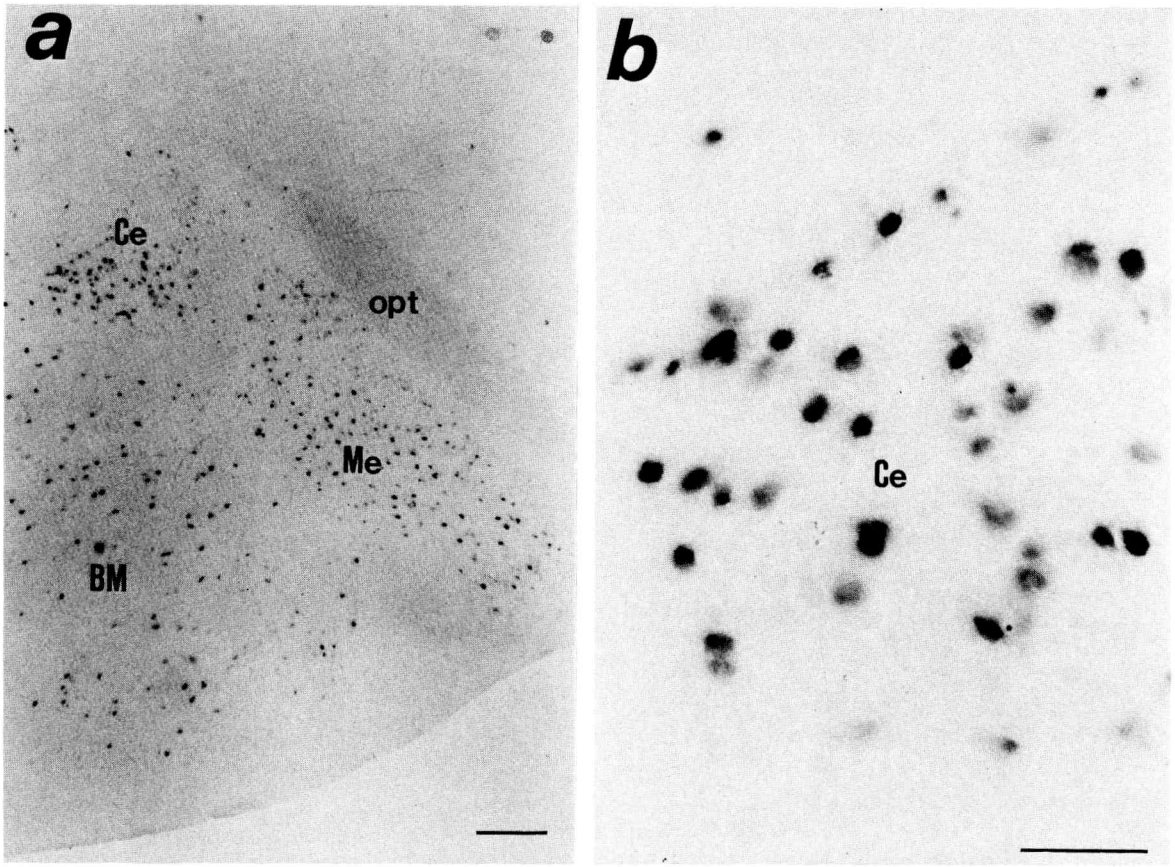

Fig. 7. The distribution of somatostatin mRNA-positive cells in amygdaloid complex. (a) Numerous somatostatin mRNA-positive cells were visualized in all parts of the amygdaloid complex; however, they were especially concentrated in the central nucleus (Ce). (b) Higher magnification of central nucleus of amygdala. Scale bars = 200 μm (a); 70 μm (b).

density of somatostatin mRNA-positive cells which were small to medium in size and contained a signal strength similar to that seen in the cells of the medial nucleus (Fig. 7a).

Caudate-putamen. Medium sized somatostatin mRNA-positive cells (15–20 μm), which contained a very intense hybridization signal, were found throughout all levels of the caudate-putamen. The density of positive cells was 5–9 cells/0.25 mm^2. Positive cells were not found in the globus pallidus.

In the entopeduncular nucleus, which is isolated in the capsule interna, 30–40 positive cells per hemisection were seen. These cells were medium in size (15–20 μm) with about 20% of positive cells containing an intense hybridization signal. The remaining cells contained a weak or moderate signal. The shape of these cells was distinctly different from those cells in the caudate-putamen with round to angular cell somata (Fig. 9).

Accumbens. In the accumbens, medium sized somatostatin mRNA-positive cells were distributed evenly throughout the nucleus with a density of 10–15 cells/0.25 mm^2. The hybridization signal in these cells was moderate to intense. One or two positive cells were also found in the anterior part of the anterior commissure and anterior commissure proper. These cells were similar in morphology to the cells in the caudate-putamen proper.

Bed nucleus of stria terminalis. In almost all areas of the bed nucleus of stria terminalis, a high density of positive cells (30–40 cells/0.25 mm^2) was found. Most of the cells contained a weak hybridization signal comparable to that seen in the lateral septum. However, some cells contained a moderate to intense signal (Fig. 5). The cells were small to medium (10–20 μm) in size and similar in morphology to the positive cells found in the central nucleus of the amygdala.

Diencephalon

Epithalamus and thalamus. In contrast to the rest of the CNS, the thalamus and epithalamus contained relatively few somatostatin mRNA-positive cells. Only a few positive cells which had a very weak signal ere found in the preoptic area, ventromedial to the dorsal lateral geniculate body, and caudal part of reticular thalamic nucleus. In the ventral region of the

thalamus, where there is an area running from the ventral part of the reticular thalamic nucleus to the zona incerta, and around these nuclei, there were a number of positive cells containing a moderate hybridization signal. These positive cells were concentrated around the zona incerta.

Hypothalamus. As would be expected from the original isolation of somatostatin from the hypothalamus, somatostatin mRNA-positive cells were distributed widely throughout the hypothalamus. The highest density of positive cells was observed in the immediate periventricular area (Figs 1a and 8a–c); however, positive cells were also observed in the periventricular area from the level of the anterior commissure downwards. At this level, 4–5 positive cells per hemi-section were found in the area adjacent to the third ventricle and above the optic nerve. The number of somatostatin mRNA-positive cells gradually increased caudally. At the level of the most rostral part of the suprachiasmatic nucleus, positive cells were found from the dorsal wall of the third ventricle to the fornix, and at the level where the caudal part of the optic chiasma was observed, the number of positive cells was maximal (at this point there were some 100–120 positive cells per hemi-section). Further, caudally at the level where the optic chiasma becomes the optic tract, the density of the cells decreased to some 10 cells per hemi-section. These cells were medium to large in size (15–30 μm) and round or oval in shape. About 90–95% of these positive cells contained a very intense hybridization signal whilst the remaining cells contained a moderate signal.

In the preoptic area, positive cells were not observed in the medial preoptic nucleus, but a few positive cells were found in the lateral preoptic nucleus in the area of medial forebrain bundle. These cells had a moderate hybridization signal.

In anterior hypothalamic nucleus and lateral hypothalamic nucleus at the same level, about 20 cells per hemi-section were found. The cells in the lateral hypothalamic nucleus contained a moderate signal, whilst those in the anterior hypothalamic nucleus contained a slightly more intense signal than those in the lateral hypothalamic nucleus.

In the suprachiasmatic nucleus, 5–7 positive cells were found per hemi-section, most of them being located on the dorsal and medial edges of this nucleus. The signal strength in these cells was moderate and less than that found in the cells of the periventricular nucleus.

The arcuate nucleus contained a large number of somatostatin-positive cells throughout its length from the level of the median eminence down to the mammillary body (Fig. 8d). About 20–25 positive cells per hemi-section were observed in this nucleus. Most of the cells were small (10–15 μm) round cells and some 90% of these cells had a moderate hybridization signal, whilst the remaining 10% had an intense signal.

The hypothalamus, at the level of the ventromedial dorsomedial nucleus (Fig. 9), also contained a moderate number of positive cells which were spread widely throughout the nuclei (5–8 positive cells/0.25 mm^2). In the dorsomedial nucleus and surrounding area, about 5–8 cells/0.25 mm^2 were observed and 30–40% of these cells had an intense hybridization signal whilst the remaining cells had a moderate signal. The size of these cells was small to medium (less than 15 μm). Only a few positive cells were observed in the ventromedial nucleus, but a moderate number of positive cells (7–10 cells/0.25 mm^2) were found in the area surrounding this nucleus, especially towards the ventral and lateral edges. These cells were mainly small, as in the dorsomedial nucleus, and 80–90% of them had a moderate hybridization signal; however, a small population of cells within this area contained an intense signal. The lateral hypothalamus, at this level, also contained a moderate density of cells (5–8 cells/0.25 mm^2) which had a similar strength of hybridization signal, comparable to that found in the cells in the surrounding area of the ventromedial nucleus.

The premammillary ventral nucleus was one of the areas which contained a very large number of positive cells. Small (less than 15 μm) positive cells were gathered in this nucleus at a density of 40–50 cells per hemi-section, and most of the cells had only a weak hybridization signal. In the regions bordering this area in the subthalamus and on the borders of the optic tract and cerebral peduncles, a few weakly stained cells were also found containing a weak hybridization signal.

Mesencephalon

Tectum. In the superior colliculus, numerous small positive cells with only a very weak hybridization signal were observed (20–30 cells/per hemi-section). Most of these cells were found in the superficial gray layer and some were also located in the intermediate gray layer (Fig. 10b).

In the inferior colliculus, numerous somatostatin-positive cells (20–30 cells/0.25 mm^2) were found which were widely distributed throughout the external cortex of inferior colliculus, although only a few of these positive cells were spread out into the central nucleus of inferior colliculus (Fig. 10a). These cells had only a very weak signal and were of uniformly small size (less than 15 μm).

Tegmentum. In the lateral tegmental area, a moderate number of somatostatin-positive cells were found which were detected in the area between the medial geniculate body and the superior colliculus and the lateral substantia nigra. Some cells were also found dorsal to this, in the substantia nigra pars compacta, although many of these positive cells had only a moderate to weak signal. Some of the cells located in the dorsomedial part of the rostral lateral substantia nigra had an intense signal. The rostral continuation

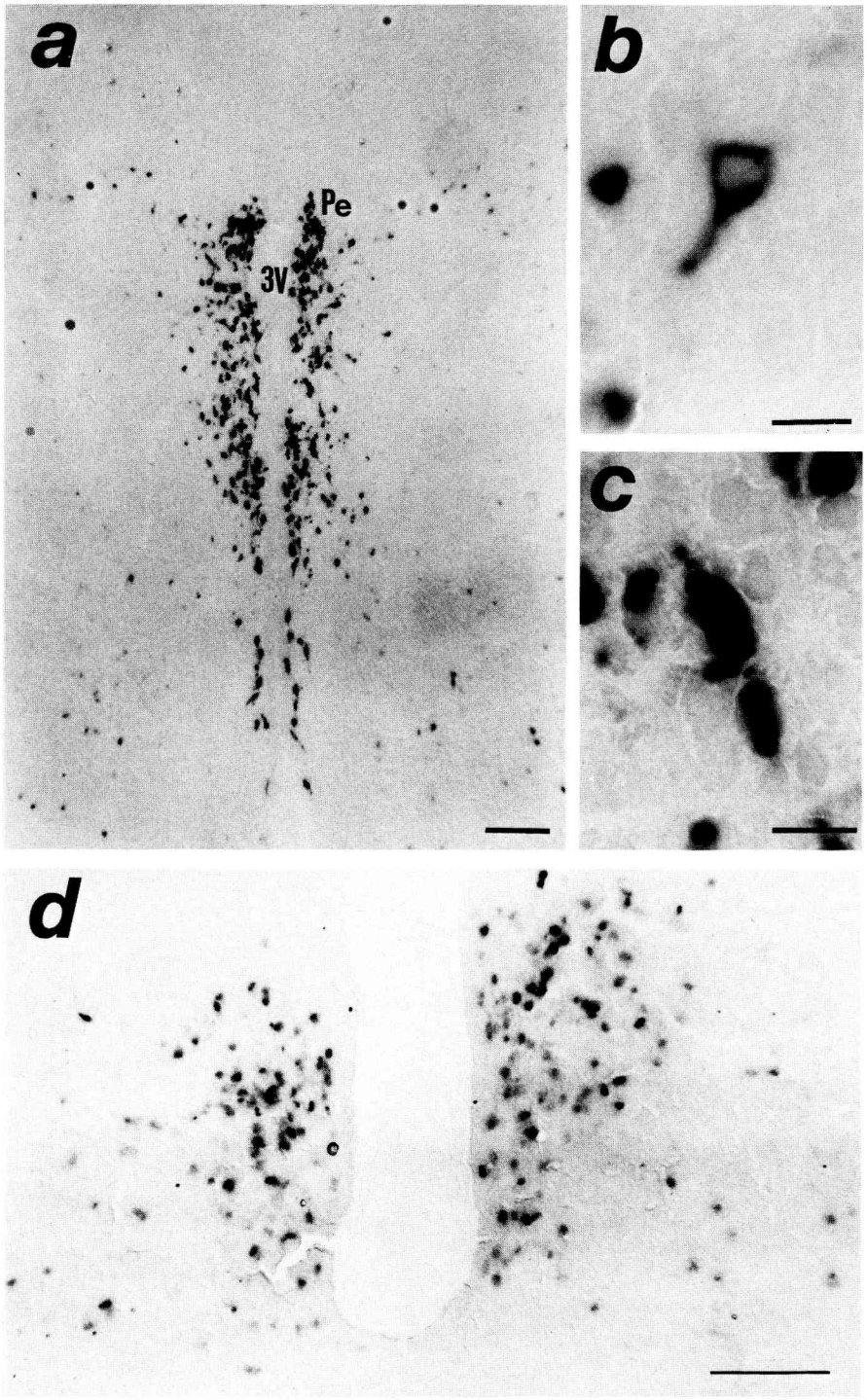

Fig. 8. Somatostatin mRNA-positive cells in periventricular area of hypothalamus. (a) Numerous somatostatin mRNA-positive cells which contained a very intense hybridization signal were concentrated in the periventricular nucleus (Pe). (b), (c) Higher magnification of the positive cells in the periventricular nucleus. The alkaline phosphatase reaction product was sometimes observed to extend out into the dendrites of these cells. (d) Caudal part of arcuate nucleus at the level of mammillary body. Scale bars = 200 μm (a); 20 μm (b, c); 150 μm (d).

of this area reached to the area dorsal to the subthalamus.

In the ventral tegmental area, the number of somatostatin mRNA-positive cells was low. In this area, between the lateral part of the supramammillary nucleus and the cerebral peduncle, a few positive cells were found. These had medium sized cell bodies (15–20 μm) and usually contained a moderate signal, with the exception of one or two isolated cells which contained an intense signal.

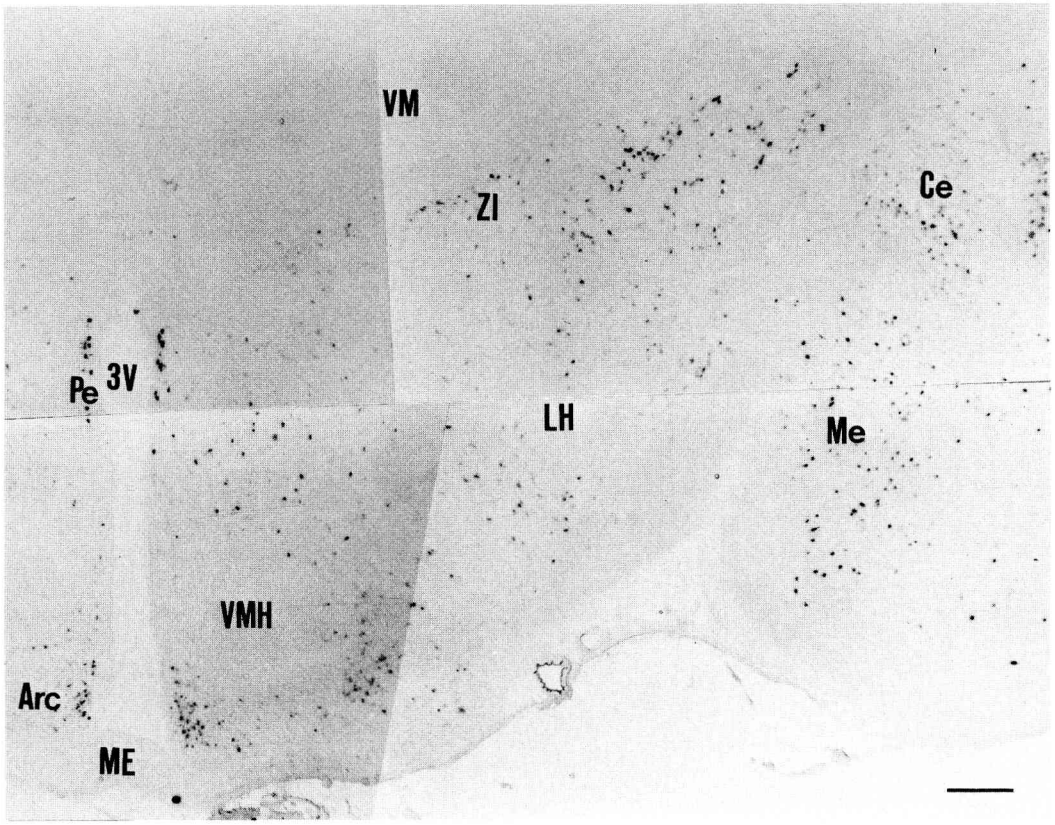

Fig. 9. Montage photomicrograph showing somatostatin mRNA-positive cells in hypothalamus at the level of the ventromedial nucleus (VMH). Note that no positive cells were detected in VMH, but a number of somatostatin mRNA-positive cells were found in other parts of the hypothalamus. Some positive cells were concentrated in zona inserta (ZI), entopeduncular nucleus, arcuate nucleus (Arc), and in the most caudal parts of the periventricular and amygdaloid nuclei. Scale bar = 400 μm.

At the level of the caudal part of the interpeduncular nucleus, where the transverse fibres of pons were first observed, there was a group of positive cells located ventrally in the interpeduncular nucleus, about 5–8 positive cells per section. These were mainly found in the dorsal part of this nucleus and had a moderate to weak hybridization signal. No positive cells were observed in the rostral part of interpeduncular nucleus.

Numerous somatostatin mRNA-positive cells were observed in central gray (20–40 cells per hemi-section). They were most concentrated in the ventrolateral part of this nucleus. In the ventral and lateral extensions of this area, including the dorsal raphe nucleus, medial longitudinal fasciculus, mesencephalic reticular area and retrorubal field, a moderate number of positive cells were also found. Almost all cells in this field had a moderate signal density. A few positive cells, again containing a moderate signal, were found in the cuneiform nucleus (Fig. 10c).

In the ventral nucleus of the lateral lemniscus, 20–30 positive cells per hemi-section were found. These had medium sized soma (20–25 μm) and contained a moderate to intense hybridization signal (Fig. 10d).

Pons. In the dorsal tegmental part of pons, a moderate number of somatostatin mRNA-positive cells were found. Somatostatin-positive cells in this area were most concentrated in the dorsal and central part of the lateral parabrachial nucleus (Fig. 11c). About 30–40 positive cells (15–25 μm) per hemi-section were found. Most of the cells contained a moderate signal, with only a few cells expressing an intense signal. The locus coeruleus contained 5–7 positive cells per hemi-section and these contained only a weak mRNA signal. A small number of positive cells were also spread out through the dorsal tegmental area of the pons, the dorsal and laterodorsal tegmental nuclei and surrounding areas. These cells also contained a weak hybridization signal. In contrast, the most caudal part of the dorsal tegmental nucleus and the supragenual nucleus contained many positive cells (about 10 positive cells per hemi-section) and these cells contained an intense hybridization signal. These positive cells continued caudally to the prepositus hypoglossal nucleus (Fig. 11d). In the prepositus hypoglossal nucleus and its ventrolateral extension, which contained the dorsal part of medial longitudinal fasciculus and dorsal paragiganto cellular nucleus, some 5–10 cells were found, although most of these cells were concentrated in the

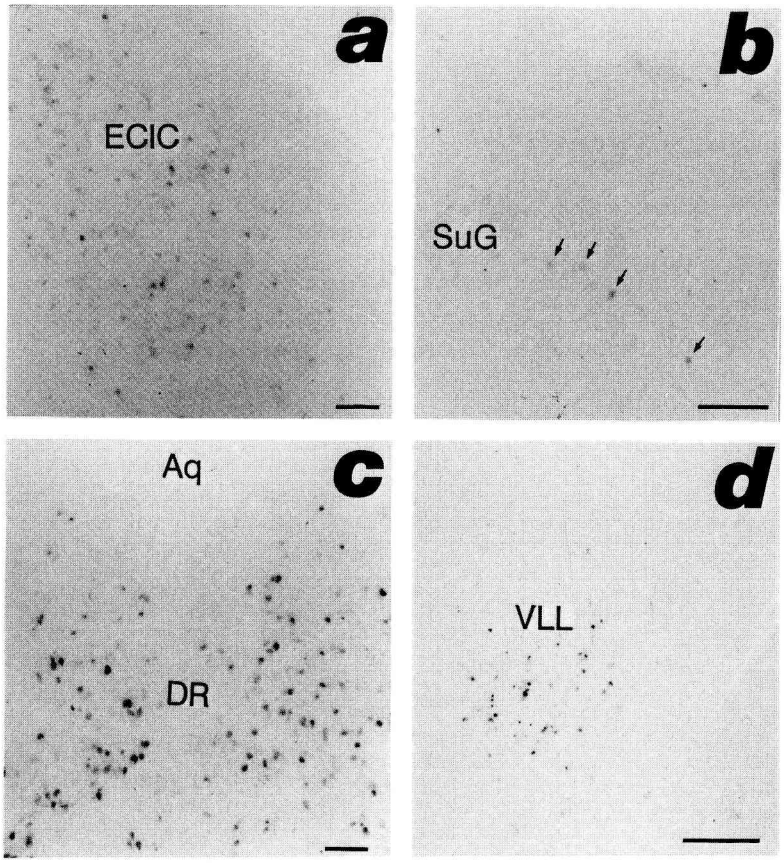

Fig. 10. Somatostatin mRNA-positive cells in the mesencephalon. (a) Many somatostatin mRNA-positive cells which contain a weak hybridization signal are located in the external cortex of the inferior colliculus (ECIC). (b) Very weakly stained cells (arrows) are located in the superficial gray layer of the superior colliculus (SuG). (c) Numerous somatostatin mRNA-positive cells are observed in the ventral part of central gray and dorsal raphe nucleus. (d) A group of somatostatin mRNA-positive cells are found in the ventral nucleus of lateral lemniscus (VLL). Scale bars = 100 μm (a–c); 300 μm (d).

prepositus hypoglossal nucleus. About 50% of these cells contained an intense mRNA signal whilst the other half had a moderate hybridization signal.

In the reticular tegmental nucleus of pons, 15–20 weakly hybridizing positive cells were found per hemi-section. These cells were medium or a little larger in size. In a part of the pontine reticular formation, which surrounds the facial nerve, medium or large positive cells (7–10 cells per hemi-section) were observed. They contained a moderate to intense hybridization signal. In other parts of the reticular formation, medial to the facial nucleus, medium sized positive cells were also found; 4–6 cells per hemi-section were observed.

The nucleus with the highest density of somatostatin mRNA-positive cells in the pons was the anterior ventral cochlear nucleus, where 50–80 positive cells per side were observed. These cells contained a weak to moderate signal (Fig. 11a,b). Although positive cells were found both in anterior and posterior ventral cochlear nucleus, the number of positive cells was much higher in the anterior, rather than in the posterior, subnucleus. We could not detect any positive cells in dorsal cochlear nucleus.

In the raphe pons only an occasional somatostatin mRNA-positive cell was observed; however, in the raphe magnus and its lateral extension 5–10 positive cells per hemi-section were observed. The positive cells in raphe magnus had medium to large cell bodies and contained a weak hybridization signal. No somatostatin mRNA-positive cells were detected in raphe pallidus.

Cerebellum. A moderate number of somatostatin mRNA-positive cells were observed in the granular layer (Fig. 12a,b). These cells were most concentrated in the medial portions of the lobules (10–15 positive cells per mm) and became distinctly less abundant in the lateral lobules. Most of these positive cells were localized in the granular layer but some positive cells were found adjacent to, or within, the Purkinje cell layer. As we could not distinguish dendritic trees of these cells it was not possible to unambiguously identify the cell types involved. However, based on their position they must include both granule and Golgi cell types. Positive cells were between 8 and 25 μm in diameter. In the paraflocculus, in contrast to the other cerebellar lobules, several positive cells were found in the Purkinje cell layer (Fig. 13). These

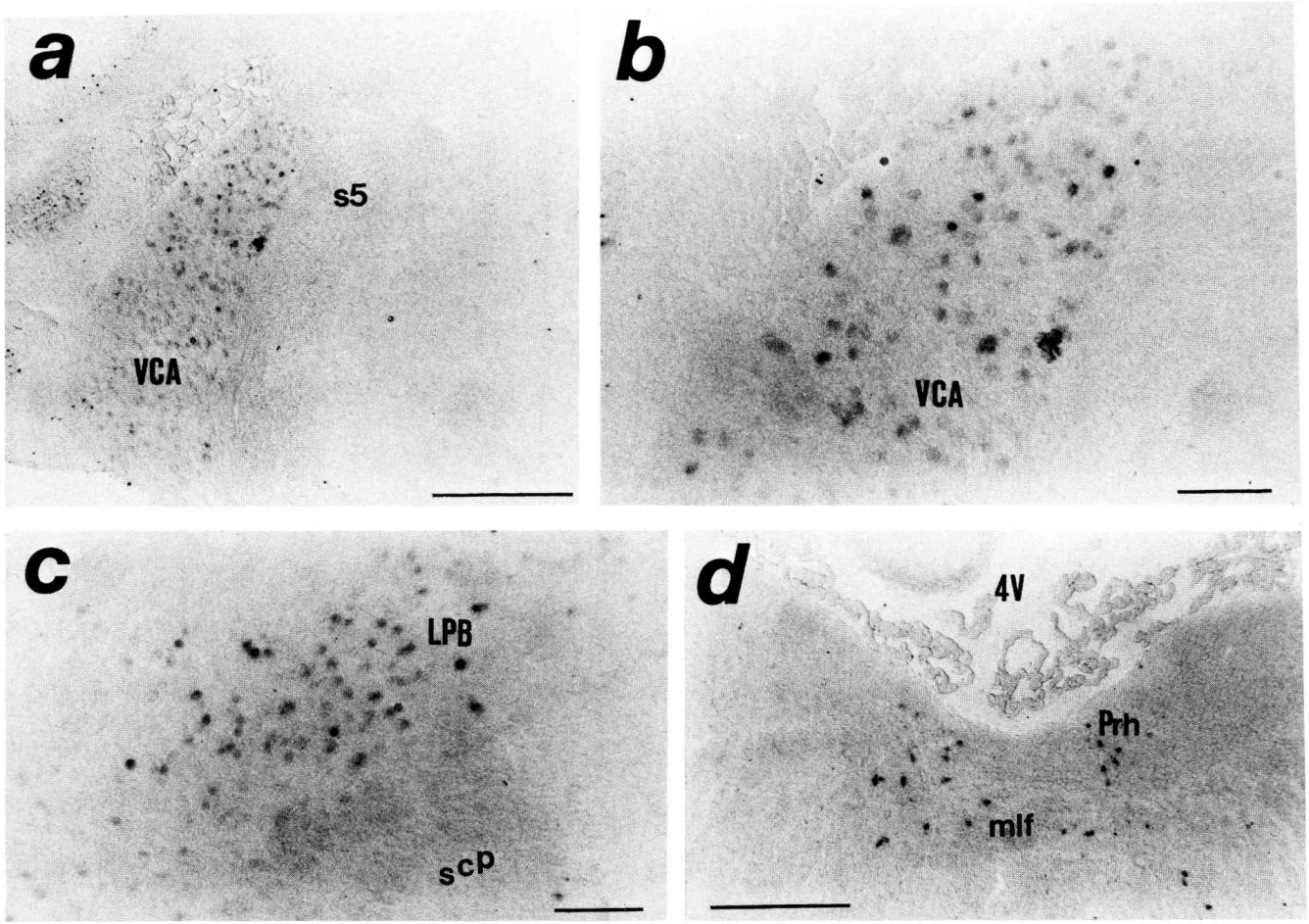

Fig. 11. Somatostatin mRNA-positive cells in pons. (a), (b) Somatostatin mRNA-positive cells were observed in the ventral cochlear nucleus pars anterior (VCA). They contained only a weak hybridization signal. (c) Somatostatin mRNA-positive cells in the lateral parabrachial nucleus. (d) Positive cells were also observed in prepositus hypoglossal nucleus (Prh) and in the medial longitudinal fasciculus (mlf). Scale bars = 200 μm (a, d); 150 μm (b, c).

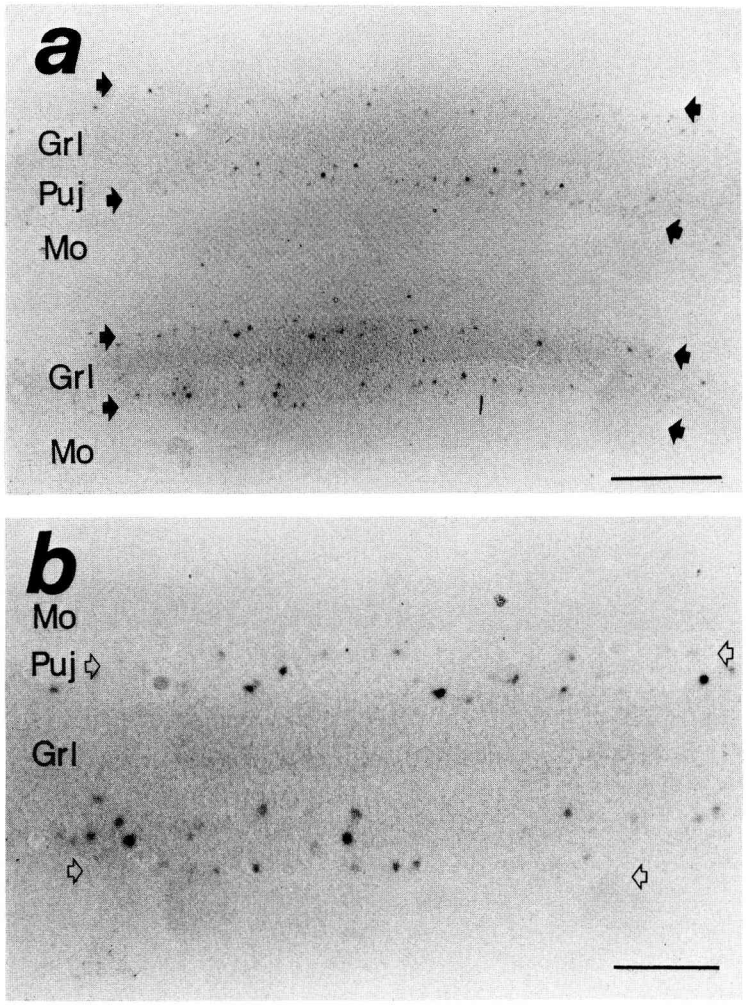

Fig. 12. Distribution of somatostatin mRNA-positive cells in cerebellum. (a) Positive cells are concentrated in the granular layer (Grl) and occasionally a positive cell was found in the Purkinje cell layer (Puj; arrow). (b) Higher magnification of (a). Scale bars = 180 μm (a); 70 μm (b).

cells were medium to large in size (20–25 μm) but contained only a weak signal. These positive cells are likely to be Purkinje cells because of their anatomical position. However, the majority of Purkinje cells in lobules other than the paraflocculus did not contain any detectable somatostatin mRNA signal. Essentially all cells detected in the cerebellum had a weak signal.

Medulla. The nuclei which contained a significant number of positive cells amongst the medullary nuclei were the solitary tract nucleus and the spinal trigeminal nucleus (Fig. 14a–c). In the rostral part of the solitary tract nucleus (Fig. 14d), 40–50 positive cells per hemi-section were visualized. They had small (7–15 μm) somata and about 20% of them contained an intense signal, whilst the other cells contained only a moderate signal. In the most rostral part of the parasolitary nucleus or nucleus Z,[37] numerous small positive cells which had a weak to moderate signal were localized in this narrow area (30–40 cells per hemi-section). Although a moderate number of positive cells existed in the caudal part of the solitary tract nucleus, both the cell density and signal strength were reduced in the caudal part of this nucleus. The commissural subnucleus, in particular, was almost devoid of positive cells. A few positive cells were found, however, in the dorsal vagal nucleus, where they seemed to be the continuation of the cell group in the solitary tract nucleus.

Both in gracile and cuneate nuclei, small positive cells were found. Gracilis contained 4–5 positive cells per hemi-section, whose hybridization signal was weak to moderate, and cuneatus had about 10 cells per hemi-section whose signal was a little stronger (about half of these contained an intense signal). A few positive cells were also found in external cuneatus and cuneate fasciculus (Fig. 14e); these were a little larger in cell size (20–25 μm) than those in the cuneate proper and contained an intense hybridization signal.

A large number of somatostatin mRNA-positive cells was seen in the spinal trigeminal nucleus, espe-

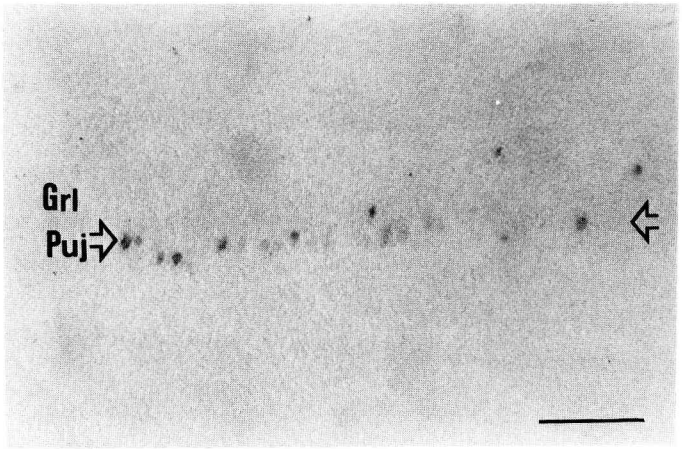

Fig. 13. Somatostatin mRNA-positive cells in the Purkinje cell layer of the paraflocculus. Somatostatin mRNA-positive cells were localized in the Purkinje cell layer (arrow) of the paraflocculus. Scale bar = 200 μm.

cially in the substantia gelatinosa of the trigeminal nucleus (Fig. 14a) which was clearly visualized in the more caudal part of the medulla (Fig. 14b). Numerous small positive cells were found to make up a tight narrow positive cell layer. The density of cells in this layer was about 20–30 per 0.5 mm. Most of these cells contained a weak signal comparable to that found in layer II of the spinal cord (see below). In the rostral and intermediate levels of the spinal trigeminal nucleus, positive cells were not evenly distributed and were much more frequent in the dorsal and ventral parts adjacent to the spinal trigeminal tract. The cellular hybridization signal in this area was generally stronger than that found in the caudal substantia gelatinosa. In the dorsal part of the spinal trigeminal tract, a few positive medium sized cells were observed. These cells were always gathered in a small area which has been termed the paratrigeminal nucleus (Fig. 14c). All of these cells had an intense signal. About 5–10 positive cells per hemi-section were present in the deepest parts of the spinal trigeminal nucleus throughout its rostrocaudal extent. They contained a moderate hybridization signal and were larger in size than the cells of the substantia gelatinosa. Similar larger cells were also found in the reticular formation just medial to the deeper part of the trigeminal nucleus.

In the ventral part of the reticular formation, some positive cells were found. A small number of cells (3–7 cells per hemi-section) were found in the lateral reticular nucleus, particularly in the medial ventral part. A few cells were also observed in the border area between the lateral reticular nucleus, the spinal trigeminal nucleus and the giganto cellular reticular nucleus. The cells distributed in this part of the reticular formation had a uniformly weak signal.

Spinal cord. Numerous small somatostatin mRNA-positive cells (50–80 cells per hemi-section) were observed, mainly concentrated in layer II, which corresponds to the substantia gelatinosa (Fig. 15). Almost all of these cells contained a weak hybridization signal. In layer X, where it surrounds the central canal, and in the medial part of layer VII which is the lateral extension of layer X, 3–5 cells were observed. About half of these medium sized cells contained a moderate signal while the others contained only a weak signal. An occasional mRNA-positive cell was found in layers III–V with a weak hybridization signal.

Sensory ganglia

Dorsal root ganglion. In the dorsal root ganglion, 10–20 intensely stained positive cells were observed per section. Most of the positive cells were medium sized and were up to 30 μm in diameter (Fig. 16a). Somatostatin mRNA-positive cells constituted about 10% of all neurons.

Trigeminal ganglion. The trigeminal ganglion, like the dorsal root ganglion, contained a number of medium sized intensely stained cells. About 8–15 positive cells/0.25 mm^2 were observed (Fig. 16).

DISCUSSION

In this study we have used a novel non-radioactive somatostatin oligonucleotide to visualize somatostatin mRNA-containing nerve cells in the adult rat brain. We chose to investigate the localization of somatostatin mRNA-containing cells because there have been a number of discrepancies between studies of the distribution of somatostatin immunoreactivity (for discussion see Vincent *et al.*[50]). It therefore seemed probable that the distribution of somatostatin-containing neurons would provide an excellent test for an *in situ* method with a wide range of cellular mRNA content and any new *in situ* method should hopefully visualize all the somatostatin cells detected by the best immunohistochemical methods. In this respect the current method is clearly successful in giving good sensitivity, low background and a better

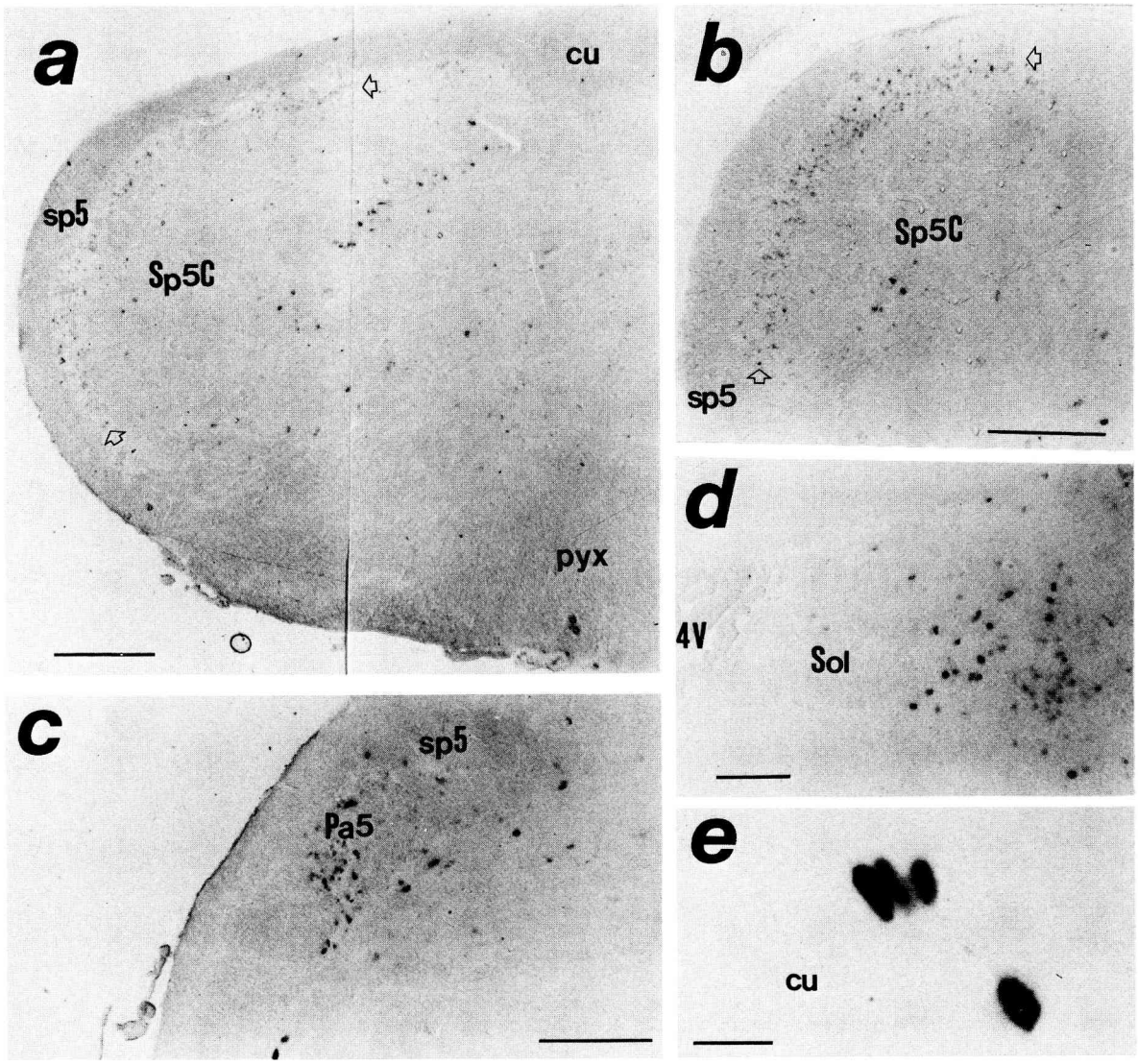

Fig. 14. Distribution of somatostatin mRNA-positive cells in the medulla. (a) Hemi-section of medulla at the level of pyramidal decussation (pyx). Numerous positive cells were observed concentrated in the substantia gelatinosa of spinal trigeminal nucleus (Sp5C). (b) Somatostatin mRNA-positive cells visualized at a slightly more caudal level than in the section shown in (a). (c) Some positive cells were present in the spinal trigeminal tract (sp5) and a moderate number of positive cells were found in the paratrigeminal tract nucleus (Pa5). (d) Somatostatin mRNA-positive cells in the solitary nucleus. (e) Higher magnification of somatostatin-positive cells in cuneate fasciculus (cu). Scale bars = 500 μm (a–c, e); 100 μm (d).

signal-to-noise ratio than observed with radioactive *in situ* protocols, as well as visualising somatostatin mRNA in cells difficult to detect by conventional immunocytochemistry. Thus, somatostatin mRNA was detected in some cells of the cerebellum which have not always yielded a positive signal in immunocytochemical studies[11,23,50] and in many areas, such as the dorsal part of lateral septum, the number of somatostatin mRNA-positive cells exceeded those previously detected by immunocytochemical studies.[11,23,50] This is probably because with conventional immunocytochemical methods, such as those using peroxidase–anti-peroxidase or avidin–biotin methods, there is a distinct background signal and it is not always easy to detect a low cellular signal. With this method the very low background with the alkaline phosphatase-labelled probe allowed us to detect mRNA-positive cells which have not previously been detected unambiguously by immunocytochemistry. Although it should be noted that this may not be a reflection of any increased sensitivity of *in situ* methods as compared with immunocytochemistry, it may indicate that some cells contain somatostatin mRNA but do not express peptide. Alternatively, there may be cells which do express the somatostatin mRNA but where the somatostatin peptide has only a short half-life, so that the mRNA but not the immunoreactive peptide is detected. Further, of course, the amount of mRNA and peptide may vary independently depending on the physiological

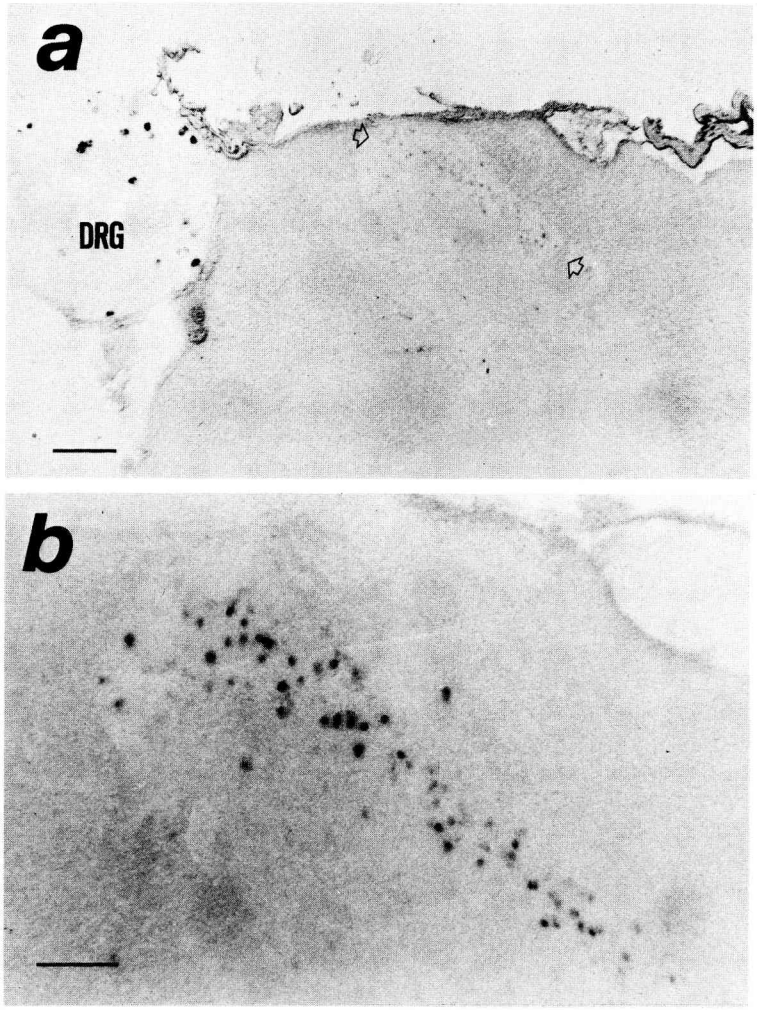

Fig. 15. Somatostatin mRNA-positive cells in the dorsal part of spinal cord. (a) Numerous positive cells were concentrated in lamina II of the substantia gelatinosa (arrows). (b) Higher magnification of (a). Scale bars = 250 μm (a); 100 μm (b).

conditions of the animal. It is particularly important to note that at no level of the rat CNS did we detect a positive signal in any control sections, in either the RNAase pretreated controls or the control sections hybridized with an excess of unlabelled oligonucleotide.

One of the reasons for the sensitivity of this method is probably the ability to continue the alkaline phosphatase reaction without an increase in background. This is a major advantage of this system over other non-radioactive methods such as those using biotinylated oligonucleotides with peroxidase or alkaline phosphatase detection[2,15,19,30] and is probably the main reason for the increased sensitivity of this method over radioactive *in situ* methods where the "background" of silver grains increases due to unavoidable exposure of emulsion-coated sections to cosmic and local radiation sources during exposure. This method also allows us to localize readily the mRNA signal within a cell; thus we could see that the mRNA signal was usually concentrated in parts of the cell cytoplasm and sometimes even to the proximal parts of the dendrites. This dendritic localization of signal was particularly noticeable in the cells of the periventricular nucleus and cerebral cortex, which contained an abundance of mRNA. Unfortunately the dendritic signal was not sufficiently strong to enable the cells to be characterized by their dendritic morphology, but it is consistent with recent reports of some mRNA being transported into dendrites.[14,43] The intensity of somatostatin mRNA signal detected by this method is in agreement with other studies of the amount and distribution of somatostatin mRNA using *in situ*, Northern or dot blot analysis.[12,16,20,34,48] It seems likely, therefore, that the amount of the cellular mRNA signal detected by this enzymatic *in situ* method is likely to be at least semi-quantitative and, in agreement with this suggestion, in an earlier study of tyrosine hydroxylase gene expression using a similar alkaline phosphatase-labelled probe this was indeed the case.[24,25] Further, the strength of alkaline phosphatase somatostatin signal detected was also in

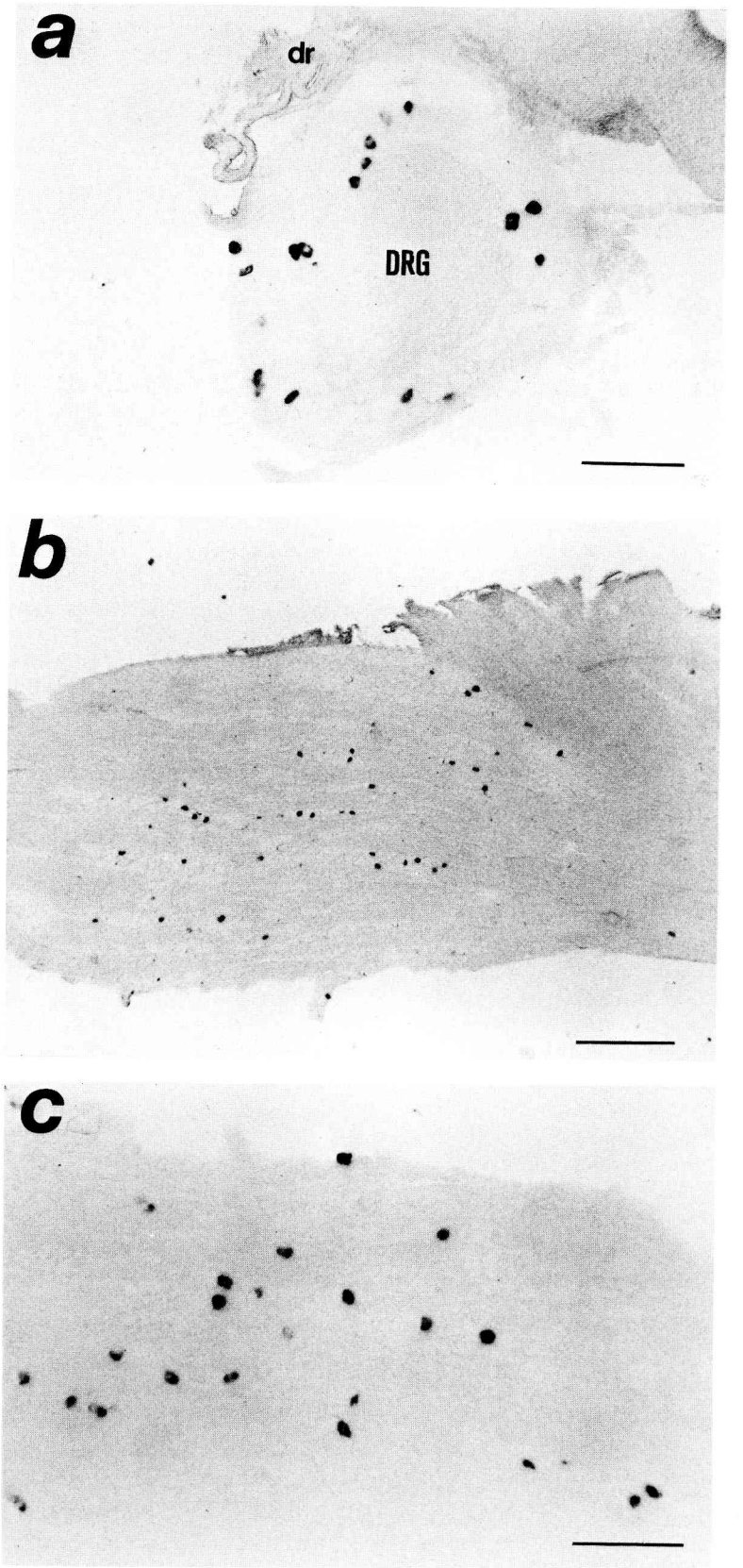

Fig. 16. The distribution of somatostatin mRNA-positive cells in sensory ganglia. (a) Dorsal root ganglion. (b) Trigeminal ganglion. (c) Higher magnification of (b). Scale bars = 170 μm (a); 400 μm (b); 180 μm (c).

good agreement with the content of somatostatin immunoreactivity observed in a number of immunocytochemical studies, i.e. those nerve cells readily detected by anti-somatostatin antibodies, which presumably contained more peptide, also usually seemed to contain more somatostatin mRNA.[12,20,34,39]

As noted earlier, this method revealed more somatostatin mRNA-positive cells than detected by most immunocytochemical studies. The reason for this may be that in areas with numerous somatostatin-positive perikarya there were no densely stained processes to obscure detection of somatostatin-positive cells. Thus in the substantia gelatinosa visualization of somatostatin mRNA-positive cells was not confused by the presence of a dense plexus of somatostatin-positive nerve endings, which may well obscure somatostatin cells when they are visualized by conventional immunocytochemistry. It is also important to note that this method does not depend on the use of a drug such as colchicine to block axonal transport and increase the cellular peptide content. Indeed, it might be seriously questioned whether, given the ability of local damage to alter expression of a number of genes (such as c-fos and many neuropeptides)[31] whose expression is influenced by Ca^{2+} and growth factors, the appearance of a positive immunocytochemical signal after local injections of compounds such as colchicine should not be considered as unequivocal evidence that a nerve cell normally expresses a particular peptide or protein.

As described in Results, we have demonstrated the localization of somatostatin mRNA-positive cells with this novel non-radioactive *in situ* method even in an area where previously there has been some discrepancy amongst those studies using immunocytochemistry and/or radioactive *in situ* hybridization histochemistry. In the accessory olfactory bulb, for example, a number of somatostatin mRNA-positive cells were visualized in the mitral cell layer. These cells are almost certainly the mitral cells because of their position, size and appearance. This observation is consistent with the immunocytochemical results of Vincent *et al.*[50] and is also the first successful demonstration of somatostatin mRNA in mitral cells. Similarly in the main olfactory bulb, many somatostatin mRNA-positive periglomerular cells were also detected. The number of positive cells found to contain somatostatin mRNA was clearly greater than previously reported,[12] but was consistent with sensitive immunocytochemical studies of Vincent *et al.*[50] In the hypothalamus, as expected, we observed a number of somatostatin-positive cells in nuclei such as the arcuate and suprachiasmatic, in good agreement with other authors.[1,3,7,23,35,36,41] In the ventromedial hypothalamus, our data again agreed well with Vincent *et al.*,[50] who noted only a few weakly stained somatostatin-containing cells. In this area we found only a few cells with a weak hybridization signal. In the superior gray layer of the superior colliculus, our results extend and confirm the two previous reports of Vincent *et al.*[50] and Fitzpatrick-McElligott *et al.*,[12] who reported the presence of somatostatin-immunoreactive and mRNA-positive cells respectively in this layer.

The area in which there has been most controversy over the localization of somatostatin cell bodies is the cerebellum, where immunocytochemical and radioactive *in situ* hybridization studies differ greatly in their findings. Amongst the *in situ* hybridization studies on somatostatin mRNA, Fitzpatrick-McElligott *et al.*[12] were not able to detect any somatostatin mRNA-positive cells in the cerebellum. In contrast, Inagaki *et al.*[20] demonstrated many mRNA-positive cells in the granule cell layer. In an immunohistochemical study Johansson *et al.*[23] reported single somatostatin-immunoreactive cells located in the Golgi cell layer, whereas Vincent *et al.*[50] reported (using a sensitive high affinity monoclonal) that they could visualize many intensely labelled Golgi cells in the granular layer, but they found only a small group of Purkinje cells, in the paraflocculus, which were immunoreactive. In almost all cerebellar lobules, we could confirm the presence of somatostatin mRNA-positive cells in the granular layer (presumably these cells are the Golgi cells described by Vincent *et al.*[50]). We also found some mRNA-positive cells in the Purkinje cell layer, but only in the paraflocculus.

CONCLUSION

Using an alkaline phosphatase-labelled antisense oligonucleotide probe we have been able to visualize somatostatin mRNA throughout the rat nervous system. The low background and high sensitivity of this novel probe suggests that this type of non-radioactive *in situ* procedure has considerable potential for the study of gene expression.

Acknowledgements—We are grateful to Mrs B. A. Oakley for typing the manuscript. H. Kiyama acknowledges the support of the Japanese Society for the Promotion of Science (JSPS), the Royal Society (U.K.) and the Association to Combat Huntington's Disease (U.K.).

REFERENCES

1. Alpert L. C., Brawer J. R., Patel Y. C. and Reichlin S. (1976) Somatostatinergic neurons in anterior hypothalamus: immunohistochemical localization. *Endocrinology* **98,** 255–258.
2. Arai H., Emson P. C., Christodoulou C. and Gait M. (1988) *In situ* hybridization histochemistry: localization of vasopressin mRNA in rat brain using a biotinylated oligonucleotide probe. *Molec. Brain Res.* **4,** 63–69.
3. Bennett-Clarke C., Romagnano M. A. and Joseph S. A. (1980) Distribution of somatostatin in the rat brain: telencephalon and diencephalon. *Brain Res.* **188,** 473–486.

4. Brazeau P., Vale W., Burgus R., Ling N., Butcher M., Rivier J. and Guillemin R. (1973) Hypothalamic polypeptide that inhibits the secretion of immunoreactive pituitary growth hormone. *Science* **197,** 77–79.
5. Brownstein M. J., Arimura A., Sato H., Schally A. V. and Kizer J. S. (1975) The regional distribution of somatostatin in the rat brain. *Endocrinology* **96,** 1456–1461.
6. Dalsgard C.-J., Hökfelt T., Johansson O. and Elde R. (1981) Somatostatin immunoreactive cell bodies in the dorsal horn and the parasympathetic intermediolateral nucleus of the rat spinal cord. *Neurosci. Lett.* **27,** 335–339.
7. Dierick K. and Van Desande F. (1979) Immunocytochemical localization of somatostatin containing neurons in the rat hypothalamus. *Cell Tiss. Res.* **201,** 349–359.
8. Dube D. and Pelletier G. (1979) Effect of colchicine on the immunohistochemical localization of somatostatin in the rat brain: light and electron microscope studies. *J. Histochem. Cytochem.* **27,** 1577–1581.
9. Epelbaum J., Arancibia L. T., Kordon C., Ottersen O. P. and Ben-Ari Y. (1979) Regional distribution of somatostatin within the amygdaloid complex of the rat brain. *Brain Res.* **174,** 172–174.
10. Finley J. C. W., Grossman G. H., Dimeo P. and Petrusz P. (1978) Somatostatin-containing neurones in the rat brain: widespread distribution revealed by immunocytochemistry after pretreatment with pronase. *Am. J. Anat.* **153,** 483–488.
11. Finley J. C. W., Maderdrut J. L., Roger L. J. and Petrusz P. (1981) The immunocytochemical localization of somatostatin-containing neurons in the rat central nervous system. *Neuroscience* **6,** 2173–2192.
12. Fitzpatrick-McElligott S., Card J. P., Lewis M. E. and Baldino F. Jr (1988) Neuronal localization of prosomatostatin mRNA in the rat brain with *in situ* hybridization histochemistry. *J. comp. Neurol.* **273,** 558–572.
13. Frossmann W. G., Burnweit C., Shehab T. and Triepel J. (1979) Somatostatin immunoreactive nerve cell bodies and fibers in the medulla oblongata et spinalis. *J. Histochem. Cytochem.* **27,** 1391–1393.
14. Garner C. C., Tucker R. P. and Matus A. (1988) Selective localization of messenger RNA for cytoskeletal protein MAP2 in dendrites. *Nature* **336,** 674–677.
15. Guitteny A.-F., Fouque B., Mougin C., Teoule R. and Bloch B. (1988) Histological detection of messenger RNAs with biotinylated synthetic oligonucleotide probes. *J. Histochem. Cytochem.* **36,** 563–571.
16. Henken D. B., Tessler A., Chesselet M. F., Hudson A., Baldino F. Jr and Murray M. (1988) *In situ* hybridization of mRNA for beta-preprotachykinin and prepro-somatostatin in adult rat dorsal root ganglia: comparison with immunocytochemical localization. *J. Neurocytol.* **17,** 671–682.
17. Hökfelt T., Elde R., Johansson O., Luft R. and Arimura A. (1975) Immunohistochemical evidence for the presence of somatostatin, a powerful inhibitory peptide, in some primary sensory neurons. *Neurosci. Lett.* **1,** 231–235.
18. Hökfelt T., Elde R., Johansson O., Luft R., Nilsson G. and Arimura A. (1976) Immunohistochemical evidence for separate populations of somatostatin-containing and substance P-containing primary afferent neurones in the rat. *Neuroscience* **1,** 131–136.
19. Ichimiya Y., Emson P. C., Christodolou C., Gait M. J. and Ruth J. (1989) Simultaneous visualization of vasopressin and oxytocin mRNA containing neurons in the hypothalamus using non-radioactive *in situ* hybridization histochemistry. *J. Neuroendocr.* **1,** 73–75.
20. Inagaki S., Shiosaka S., Sekitani M., Noguchi K., Shimada S. and Takagi H. (1989) *In situ* hybridization analysis of the somatostatin-containing neuron system in developing cerebellum of rats. *Molec. Brain Res.* **6,** 289–295.
21. Inagaki S., Shiosaka S., Takatsuki K., Iida H., Sakanaka M., Senba E., Hara Y., Matsuzaki T., Kawai Y. and Tohyama M. (1982) Ontogeny of somatostatin-containing neuron system of the rat cerebellum including its fiber connections: an experimental and immunohistochemical analysis. *Devl Brain Res.* **3,** 509–527.
22. Jablonski E., Moomaw E. W., Tullis R. H. and Ruth J. (1986) Preparation of oligodeoxynucleotide–alkaline phosphatase conjugates and their use as hybridization probes. *Nucleic Acid Res.* **14,** 6115–6128.
23. Johansson O., Hökfelt T. and Elde R. P. (1984) Immunohistochemical distribution of somatostatin-like immunoreactivity in the central nervous system of the adult rat. *Neuroscience* **13,** 265–339.
24. Kiyama H., Emson P. C., Ruth J. and Morgan C. Y. (1990) Sensitive non-radio isotopic *in situ* hybridization histochemistry: demonstration of tyrosine hydroxylase gene expression in rat brain and adrenal. *Molec. Brain Res.* **7,** 213–219.
25. Kiyama H., Ruth J. and Emson P. C. (1989) Cellular localization of tyrosine hydroxylase mRNA in the rat brain and adrenal medulla. *Br. J. Pharmac.* **97,** 476P.
26. Kiyama H., Ruth J. and Emson P. C. (1989) The detection of somatostatin gene expression by non-radioisotopic *in situ* hybridization histochemistry. *Eur. J. Neurosci. Suppl.* **2,** 204.
27. Kohler C. and Chan-Palay V. (1982) Somatostatin-like immunoreactive neurons in the hippocampus: an immunocytochemical study in the rat. *Neurosci. Lett.* **34,** 259–264.
28. Kohler C. and Eriksson L. G. (1984) An immunohistochemical study of somatostatin and neurotensin positive neurons in the septal nuclei of the rat brain. *Acta Embryol.* **170,** 1–10.
29. Krisch B. (1978) Hypothalamic and extra hypothalamic distribution of somatostatin immunoreactive elements in the rat brain. *Cell Tiss. Res.* **195,** 499–513.
30. Lewis F. A., Griffiths S., Dunnicliff R. and Wells M. (1987) Sensitive *in situ* hybridization technique using biotin–streptavidin polyalkaline phosphatase complex. *J. clin. Path.* **40,** 163–166.
31. Morgan J. I. and Curran T. (1988) Calcium as a modulator of the immediate–early gene cascade in neurons. *Cell Calcium* **9,** 303–311.
32. Morrison J. H., Benoit R., Magistretti P. J. and Bloom F. E. (1982) Immunohistochemical distribution of pro-somatostatin-related peptides in cerebral cortex. *Brain Res.* **262,** 344–351.
33. Morrison J. H., Benoit R., Magistretti P. J., Ling N. and Bloom F. E. (1982) Immunohistochemical distribution of pro-somatostatin related peptides in hippocampus. *Neurosci. Lett.* **34,** 137–142.
34. Naus C. C. S., Miller F. D., Morrison J. H. and Bloom F. E. (1988) Immunohistochemical and *in situ* hybridization analysis of the development of the rat somatostatin-containing neocortical neuronal system. *J. comp. Neurol.* **269,** 448–463.
35. Ohtsuka M., Hisano S. and Daikoku S. (1983) Electron-microscopic study of somatostatin-containing neurones in rat arcuate nucleus with special reference to neuronal regulation. *Brain Res.* **263,** 191–199.
36. Parsons J. A., Erlandson S. L., Hegre P., McEvoy O. D. and Elde R. P. (1976) Central and peripheral localization of somatostatin: immunoenzyme immunocytochemical studies. *J. Histochem. Cytochem.* **24,** 872–882.
37. Paxinos G. and Watson C. (1986) *The Rat Brain in Stereotaxic Coordinates*, 2nd edn. Academic Press, London.

38. Ruth J., Morgan C. and Pasko A. (1985) Linker arm nucleotide analogs useful in oligonucleotide synthesis. *DNA* **4,** 93.
39. Sekitani M., Shiosaka S., Kuriyama H., Lee Y., Ikeda M. and Tohyama M. (1990) Transient expression of somatostatin mRNA in the auditory system of the neonatal rat. *Molec. Brain Res.* **7,** 177–181.
40. Senba E., Shiosaka S., Hara Y., Inagaki S., Sakanaka M., Takatsuki K., Kawai Y. and Tohyama M. (1982) Ontogeny of the peptidergic system in the rat spinal cord: immunohistochemical analysis. *J. comp. Neurol.* **208,** 54–66.
41. Shiosaka S., Takatsuki K., Sakanaka M., Inagaki S., Takagi H., Senba E., Kawai Y., Minagawa H. and Tohyama M. (1981) New somatostatin-containing sites in the diencephalon of neonatal rat. *Neurosci. Lett.* **25,** 69–73.
42. Shiosaka S., Takatsuki K., Sakanaka M., Inagaki S., Takagi H., Senba E., Kawai Y. and Tohyama M. (1981) Ontogeny of somatostatin-containing neuron system of the rat: immunohistochemical analysis. II. Forebrain and diencephalon. *J. comp. Neurol.* **204,** 211–224.
43. Steward O. and Falk P. M. (1986) Protein-synthetic machinery at postsynaptic sites during synaptogenesis: a quantitative study of the association between polyribosomes and developing synapses. *J. Neurosci.* **6,** 412–423.
44. Tachibana M., Rothman J. M. and Guth P. S. (1979) Somatostatin along the auditory pathway. *Hearing Res.* **1,** 365–368.
45. Takatsuki K., Sakanaka M., Shiosaka S., Inagaki S., Takagi H., Senba E., Hara Y., Kawai Y., Minagawa H., Iida H. and Tohyama M. (1982) Pathway and terminal fields of the cochlear fugal somatostatin tracts of very young rats. *Devl Brain Res.* **3,** 613–626.
46. Takatsuki K., Shiosaka S., Sakanaka M., Inagaki S., Senba E., Takagi H. and Tohyama M. (1981) Somatostatin in the auditory system of the rat. *Brain Res.* **213,** 211–216.
47. Uhl G. R. (1986) In Situ *Hybridization in Brain.* Plenum Press, New York.
48. Uhl G. R. and Sasek C. A. (1986) Somatostatin mRNA: regional variation in hybridization densities in individual neurons. *J. Neurosci.* **6,** 3258–3264.
49. Valentino K. L., Eberwine J. H. and Barchas J. D. (1987) In Situ *Hybridization: Application to Neurobiology.* Oxford University Press, Oxford.
50. Vincent S. R., McIntosh C. H. S., Buchan A. M. J. and Brown J. C. (1985) Central somatostatin systems revealed with monoclonal antibodies. *J. comp. Neurol.* **238,** 169–186.

(*Accepted* 30 *April* 1990)

Journal of Neuroendocrinology, Vol. 2, No. 3

RAPID COMMUNICATION

Evidence for the Co-Expression of Oxytocin and Vasopressin Messenger Ribonucleic Acids in Magnocellular Neurosecretory Cells: Simultaneous Demonstration of Two Neurohypophysin Messenger Ribonucleic Acids by Hybridization Histochemistry

Hiroshi Kiyama and Piers C. Emson

MRC Group, AFRC Institute of Animal Physiology and Genetics Research, Babraham, Cambridge CB2 4AT, UK.

Key words: oxytocin, vasopressin, messenger ribonucleic acid 'co-expression', salt loading.

A novel enzyme-labelled oligonucleotide probe specific for oxytocin messenger ribonucleic acid (mRNA) and a radiolabelled oligonucleotide probe specific for vasopressin mRNA were used together to visualize both oxytocin and vasopressin mRNA's in hypothalamus sections from salt loaded (2% saline) rats. The results demonstrate that the majority of magnocellular neurons contain only oxytocin or vasopressin mRNA, however a small number of neurons, 1% to 2%, contained both oxytocin and vasopressin transcripts.

In situ hybridization histochemistry is a method which can be used to demonstrate the cellular localization of an mRNA signal (1). There are a number of variations on this method, but most procedures employ radiolabelled complementary DNA or RNA probes which can only be visualized by autoradiography. Autoradiographic procedures used on their own are not well suited to studies of the possible co-existence or co-expression of two mRNAs in one cell and in order to do this either a combination of radiolabelled and non-radiolabelled complementary probes (2), or a combination of two non-radiolabelled probes which can be detected by different coloured reporter molecules has to be used (3). In an initial study using two non-radioactive *in situ* probes (3) we found that the majority (>95%) of magnocellular neurosecretory cells in osmotically-stressed rats contained only one transcript (either oxytocin or vasopressin). However, there were a small number of cells where we could not be certain using our two colour detection system, whether the cells might possibly contain both transcripts.

In order to clarify this important point we have now used a combination of a [^{35}S]radiolabelled antisense vasopressin probe specific for the glycopeptide sequence of vasopressin neurophysin not present in the oxytocin mRNA and an alkaline phosphatase-labelled antisense oligonucleotide probe specific for a 5′ sequence of oxytocin which did not detect vasopressin mRNA (for details see legends to Figs. 1 and 2). In double-labelling experiments the two specific probes were applied simultaneously to hypothalamic sections from control and osmotically-stressed male rats (2% saline in the drinking water for 2 weeks). After an appropriate stringent washing of the sections, the sections were first incubated in the alkaline phosphatase substrate to visualize the sites of oxytocin mRNA expression. Once the colour development was

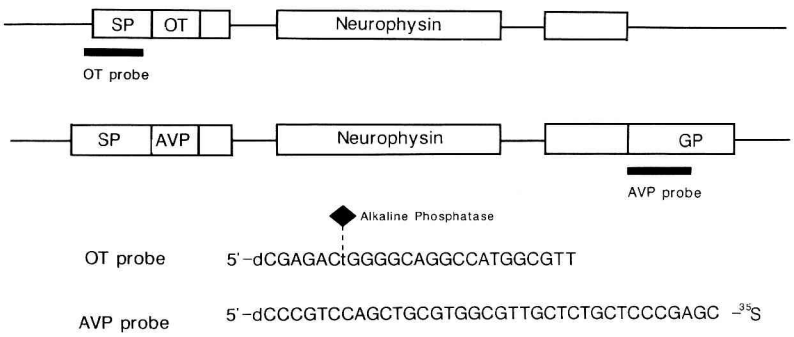

FIG. 1. The strategy for demonstrating two mRNAs in a single section. The sequences of the probes were selected to avoid possible cross-reaction as the two genes (vasopressin, AVP or oxytocin, OT) have a considerable degree of sequence similarity especially in the regions coding for the hormone and neurophysins. The OT probe sequence was selected from the 5′-part of the signal peptide, and the AVP sequence was derived from the sequence coding for the first 12 amino-acids of the glycopeptide (not present in the OT transcript). In order to demonstrate the two mRNAs, two different labelling methods were used. Here we employed a novel sensitive non-radioactive *in situ* hybridization method for the detection of the OT mRNA and a conventional radioactive detection method for AVP mRNA. The probe for OT mRNA was labelled with alkaline phosphatase (4, 5). This probe has previously been shown to give a high resolution and high sensitivity in detecting OT mRNA (3). The AVP antisense probe was [^{35}S]labelled using terminal deoxynucleotidyl transferase. After alkaline phosphatase detection (OT mRNA) sections were dipped in autoradiography emulsion, and subsequently developed to visualize the [^{35}S]labelled AVP mRNA signal. SP—signal peptide; GP—glycopeptide.

Correspondence to: P. C. Emson, MRC Group, AFRC Institute of Animal Physiology and Genetics Research, Babraham, Cambridge CB2 4AT, UK.

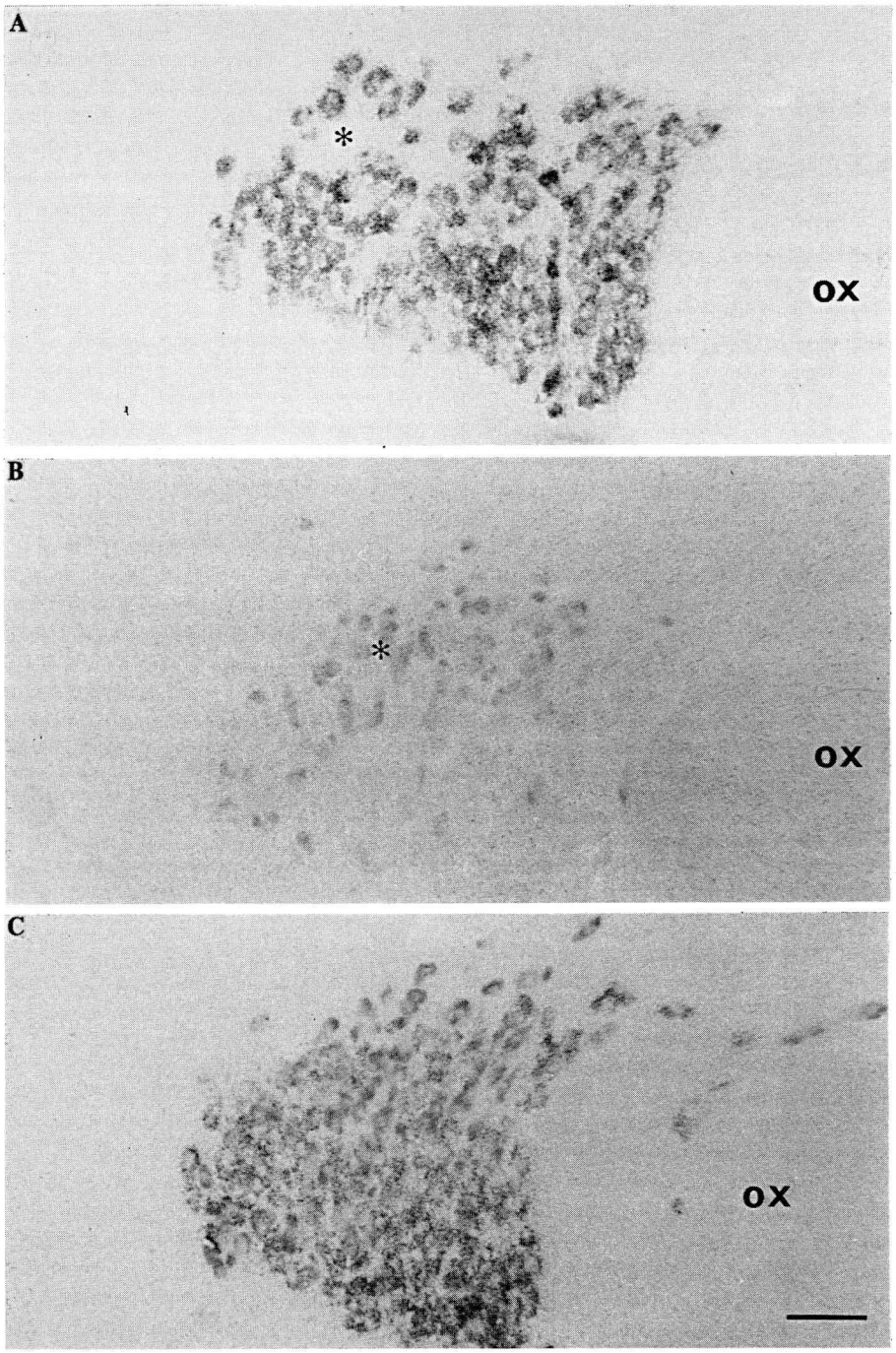

FIG. 2. The histological specificities of the probes were checked with several control experiments. First, ribonuclease (RNaseA) pretreatment was used. This treatment digests any mRNA signal in the section and was carried out just before incubating the sections for hybridization (see Fig. 3). This was a check that neither the alkaline phosphatase oligonucleotide nor the [^{35}S]labelled oligonucleotide were binding non-specifically to the tissue section or slide. After RNase A pretreatment (20 μg/ml) for 30 min at room temperature we could not demonstrate any specific oxytocin (OT) or vasopressin (AVP) mRNA signal on the sections. As a further control, competition experiments were carried out on serial sections (A and B). Excess non-labelled oligonucleotide probe (200 fmol/μl) for OT was added to the hybridization buffer which contained both alkaline phosphatase-labelled OT probe (2 fmol/μl) and [^{35}S]labelled AVP probe (2 fmol/μl). The non-labelled OT probe competed with the alkaline phosphatase-labelled OT probe and abolished the OT signal, but did not influence the detection of the radiolabelled AVP probe (A; silver grains over labelled cells show AVP mRNA positive cells in supraoptic nucleus). Similarly an excess of non-labelled AVP probe (200 fmol/μl) was added to the hybridization buffer. In this case the radioactive AVP signal was not detectable but the OT alkaline phosphatase signal was readily visualized (B). (C) shows a third serial section hybridized without either competing probe. The stars in (A) and (B) are located in the same position in the supraoptic nucleus and correspond to an area rich in OT cells but not containing AVP cells. Finally, in order to rule out the possibility that we were detecting overlapping cells in a section, we used two consecutive serial sections and hybridized these at the same time. In these cases, some double-labelled cells were found in the same position on both sections, and these were believed to represent two halves of one single cell, one half being present on each side of the 10 μm sections. (For the hybridization method see Fig. 3). OX—optic chiasma. Bar: 100 μm.

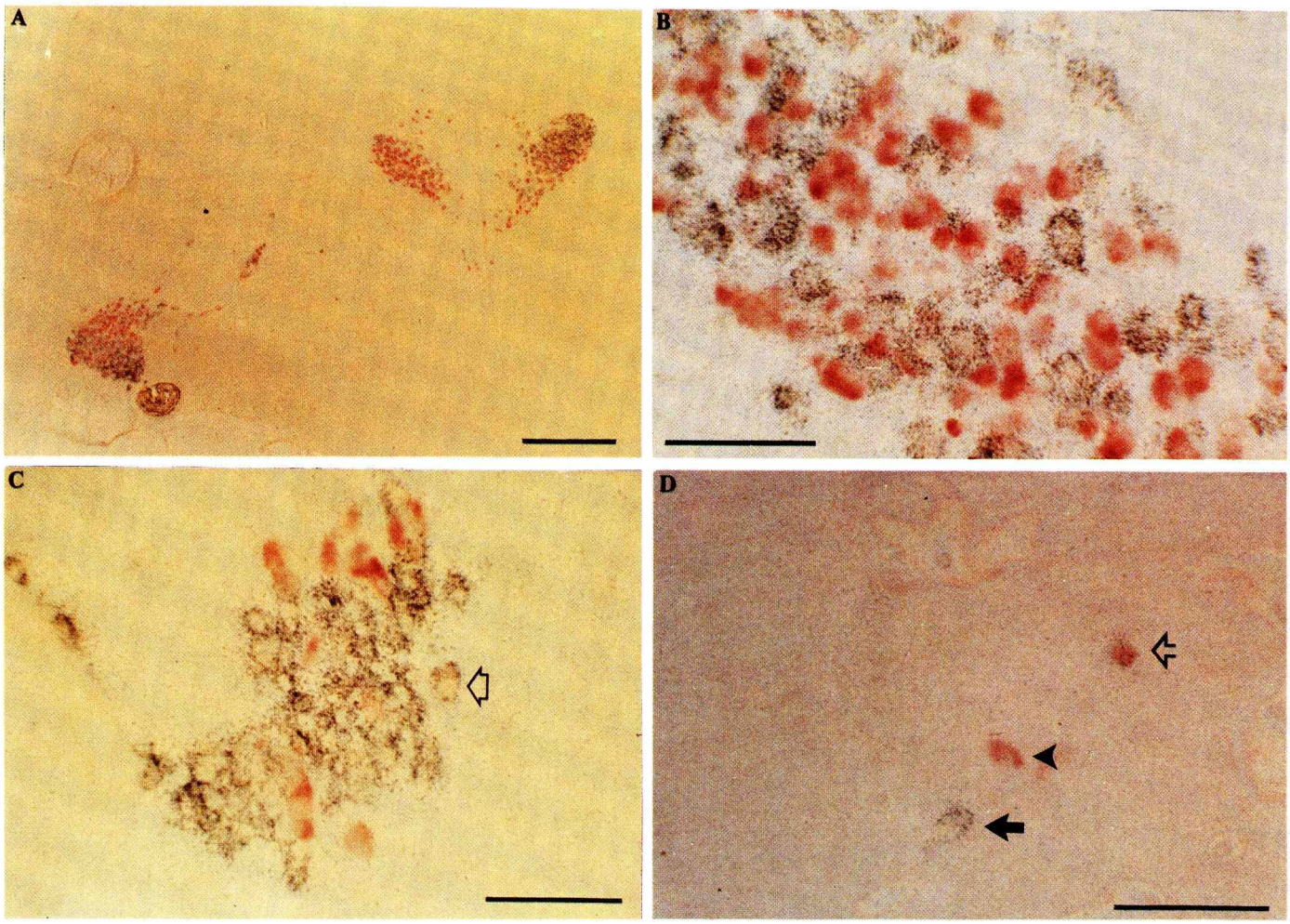

FIG. 3. *In situ* hybridization of vasopressin (AVP) and oxytocin (OT) probes to demonstrate the use of the double-labelled *in situ* procedure and the presence of the two mRNAs (AVP and OT) in some neurosecretory cells. (A) Low magnification of the hypothalamic area containing both the paraventricular nucleus and supraoptic nucleus. The red cells are OT mRNA positive cells detected by the alkaline phosphatase-labelled probe and the black silver grains visualize those cells containing AVP mRNA. (B) A higher magnification of the paraventricular nucleus. In this section there are no unambiguously identifiable double-labelled cells and the specificity of the probes for OT and AVP mRNAs is clear. (C) A higher magnification of the supraoptic nucleus. The open arrow shows a cell which clearly contains both a red signal corresponding to OT mRNA and silver grains corresponding to the AVP mRNA. (D) Brightfield illumination and (E) darkfield illumination of the same section shows an example of a double-labelled and two single-labelled cells in the accessory nucleus. The open arrow shows a double-labelled cell, the filled arrow shows a cell with silver grains (AVP mRNA) only, and the arrowhead shows a cell with only the red signal which corresponds to OT mRNA.

METHODS. Fresh frozen sections (10 μm thickness) were cut on a cryostat and fixed with 4% paraformaldehyde in 0.1 M phosphate buffer for 30 min at room temperature. Fixed sections were then rinsed twice with 0.1 M phosphate-buffered saline and incubated in 0.25% acetic anhydride in 0.1 M triethanolamine/0.9% NaCl for 10 min at room temperature. Sections were dehydrated with 70%, 80%, 90%, 95% and absolute ethanol for 5 min each, then delipidated in chloroform for 10 min and again washed with absolute ethanol. Dried sections were hybridized in the following hybridization buffer; 4 × SSC, 50% formamide, 1 × Denhardt's solution, 500 μg/ml sheared salmon testis DNA, 10% dextran sulfate and probes. The probes for OT and AVP mRNAs were added to the hybridization buffer at the same time. The concentration of both probes was approximately 2 fmol/μl. The hybridization buffer which contained the two probes was then poured on to the slide. Hybridization was carried out overnight at 37 °C in a moist box. After hybridization, the sections were quickly washed with 4 × SSC to remove the hybridization buffer on the sections, and then stringently washed with 1 × SSC at 55 °C, three changes each of 20 to 30 min. Finally, the sections were washed with 1 × SSC for 1 h at room temperature. After washing, the colour development for alkaline phosphatase was carried out. In order to change the buffer conditions, sections were incubated in 0.1 M Tris HCl buffer (pH 7.5) containing 0.9% NaCl for 30 min at room temperature, and then incubated in high alkaline buffer (0.1 M Tris HCl, pH 8.2) for 10 min. The Vector red (Vector Labs, Peterborough, UK) was used as the alkaline phosphatase substrate. Sections were incubated in the substrate solution overnight and the reaction was terminated by washing with 10 mM Tris HCl containing 10 mM EDTA and 0.9% NaCl for 2 h. The sections were then dried after a quick wash in 70% ethanol and then dipped in emulsion (Ilford K-5) for detection of the [^{35}S]labelled AVP mRNA signal. These sections were exposed for 10 days in a dark box, developed for 2.5 min in D19 developer (Kodak) and then fixed. After washing the sections with tap water for 30 min they were coverslipped in 10 mM Tris HCl containing 10 mM EDTA and 50% glycerol. Bar: (A) 400 μm, (B–E) 100 μm.

complete sections were then washed, dried and dipped in autoradiography emulsion to detect the antisense [^{35}S]labelled vasopressin probe (for details see legends to Figs. 1 and 2). Emulsion-dipped sections were exposed in the dark for an appropriate time and the signal corresponding to the vasopressin transcript was then detected (silver grains). Detailed examination of the double-labelled sections revealed that although the majority of magnocellular cells contained only one transcript, either vasopressin or oxytocin, there were a number of double-labelled cells in the caudal part of the supraoptic nucleus (SO) and in the accessory nucleus. In contrast, only occasional double-labelled cells were found in the paraventricular nucleus (3 cells out of 499 which contained an oxytocin signal also contained a vasopressin signal). The double-labelled cells in SO were found mainly on the lateral and ventral borders of the nucleus and constituted not more than 1% to 2% of the total number of supraoptic magnocellular cells (12 cells out of 504 which contained oxytocin also contained a vasopressin signal). In the more rostral parts of SO we did not detect any double-labelled cells. In non-salt loaded control rats a few double-labelled cells were detected ($< 1\%$ of the magnocellular cells) but as noted their number was substantially increased by osmotic stress (Fig. 3).

One previous study which examined this point using double-labelling with biotinylated and radiolabelled *in situ* probes did not detect any co-expression of both oxytocin and vasopressin transcripts under similar conditions of osmotic stress (2). The reason for this difference in findings is almost certainly due to the much improved sensitivity we obtained using an enzyme-labelled, rather than biotinylated probe. Indeed, our experience comparing the sensitivity of biotinylated versus enzyme-labelled probes suggests that the enzyme-labelled probes may be at least as sensitive as radiolabelled probes for *in situ* experiments (6). As discussed by Mohr and colleagues (2) both the oxytocin and vasopressin genes are localized close to each other in the rat genome and they contain a number of similar upstream regulatory elements capable of responding to glucocorticoids or oestrogens for example. It remains to be established why a small subpopulation of oxytocin/vasopressin cells express both transcripts, but it is clear that under the conditions of osmotic stress used here the majority of cells express only one transcript. It would also be very interesting to know if the small percentage of double-labelled cells we have identified correspond to those few SO cells which have the electrophysiological characteristics of vasopressin cells but also show the functional characteristics of oxytocin cells (7). Similarly, it would be of some interest to know if these cells can process both transcripts into their respective neurohormones and associated neurophysins. In view of the difficulty of possible cross-reactions in immunocytochemical studies with neurohormone- or neurophysin-directed antisera such a study may not be feasible. Indeed, under these circumstances the '*in situ*' results are likely to be more specific.

Acknowledgements

H. K. is a Fellow of the Japanese Society for the Promotion of Science (JSPS). We are grateful to Dr J. Ruth and Ms C. Morgan for the provision of the enzyme-labelled oxytocin oligonucleotide and to Dr G. Leng for his advice and helpful comments on this study.

Accepted 20 February 1990

References

1. Uhl GR. (1986). **In situ hybridisation in brain.** Plenum Press, New York.
2. Mohr E, Bahnsen U, Kiessling C, Richter D. (1988). Expression of the vasopressin and oxytocin genes in rats occurs in mutually exclusive sets of hypothalamic neurons. **FEBS Lett.** 242: 144–148.
3. Ichimiya Y, Emson PC, Christodoulou C, Gait MJ, Ruth JL. (1989). Simultaneous visualization of vasopressin and oxytocin mRNA-containing neurons in the hypothalamus using non-radioactive *in situ* hybridization histochemistry. **J Neuroendocrinol.** 1: 73–75.
4. Jablonsky E, Moomaw EW, Tullis RH, Ruth JL. (1986). Preparation of oligodeoxynucleotide-alkaline phosphatase conjugates and their use as hybridisation probes. **Nucleic Acids Res.** 14: 6115–6128.
5. Ruth J, Morgan C, Pasko A. (1985). Linker arm nucleotide analogs useful in oligonucleotide synthesis. **DNA.** 4: 93.
6. Kiyama H, Emson PC, Ruth J, Morgan C. (1990). Sensitive non-radioactive in situ hybridisation histochemistry: demonstration of tyrosine hydroxylase gene expression in rat brain and adrenal. **Mol Brain Res.** 6: 213–219.
7. Lincoln D, Wakerley JB. (1974). Electrophysiological evidence for the activation of supraoptic neurones during the release of oxytocin. **J Physiol.** 242: 533–554.